Wave data analysis for a semi-sheltered site in the Inner Hebrides of Scotland suitable for small scale WEC development

Elsevier Editorial System(tm) for Ocean Engineering

Manuscript Draft

Manuscript Number: OE-D-16-00255R3

Title: Wave data analysis for a semi-sheltered site in the Inner Hebrides of Scotland suitable for small scale WEC development

Article Type: Full length article

Keywords: Wave Power; Aquaculture; ADCP; Wave buoy; Swell; Wind Sea

Corresponding Author: Mr. Arne Vogler,

Corresponding Author's Institution:

First Author: Arne Vogler

Order of Authors: Arne Vogler; Vengatesan Venugopal

Abstract: Wave data analysis from a short-term deployment of a wave buoy and AWAC in the lee of a Hebridean island in the United Kingdom is discussed in this paper. Significant parameters are calculated and Rayleigh, Weibull and Kernel density probability distributions have been employed to fit the measured data. Results show that while the Atlantic facing side of the island is exposed to a predominant swell based wave regime, the area in the lee features bimodality for wave period and directionality. The Kernel density distribution is found to fit the measured bimodality well compared to Rayleigh and Weibull distributions. The analysis illustrates that interference between swell waves and associated wave periods from north with southerly wind driven seas creates a complex sea state. It is shown that the higher wind sea related frequency components are of more significance in the lee of the island than at the open ocean site. Findings of this study are relevant to the aquaculture sector or small scale wave energy developers (e.g. <100 kW), as an insight is provided into the interaction between ocean swell and localised wind seas in semi-sheltered areas.

Highlights

- Compares wave data from bottom deployed acoustic sensor and floating buoy
- Observes bimodality for wave period and directionality in lee off an island as a result of diffracted/refracted swell waves and localised wind seas
- Considers relevance of findings to aquaculture and wave power sectors
- Suggests possible exclusion of frequencies of the wave spectrum that are not contributing to energy production from specific WEC types from spectral sea state analysis
- Applies Weibull, Rayleigh and Kernel density estimation to fit wave height and period distributions

Wave data analysis for a semi-sheltered site in the Inner Hebrides of Scotland suitable for small scale WEC development

Authors:

1. Arne Vogler, Marine Energy Research Group, Lews Castle College, University of the Highlands and Islands, Stornoway, Isle of Lewis, Scotland, GB-HS2 0XR, arne.vogler@uhi.ac.uk

2. Vengatesan Venugopal, School of Engineering, The University of Edinburgh, Faraday Building, King's Buildings, Colin Maclaurin Road, Edinburgh, UK, EH9 3DW, V.Venugopal@ed.ac.uk

Corresponding author: Arne Vogler, +44(0)1851 770 325, e-mail: arne.vogler@uhi.ac.uk

Abstract

Wave data analysis from a short-term deployment of a wave buoy and AWAC in the lee of a Hebridean island in the United Kingdom is discussed in this paper. Significant parameters are calculated and Rayleigh, Weibull and Kernel density probability distributions have been employed to fit the measured data. Results show that while the Atlantic facing side of the island is exposed to a predominant swell based wave regime, the area in the lee features bimodality for wave period and directionality. The Kernel density distribution is found to fit the measured bimodality well compared to Rayleigh and Weibull distributions. The analysis illustrates that interference between swell waves and associated wave periods from north with southerly wind driven seas creates a complex sea state. It is shown that the higher wind sea related frequency components are of more significance in the lee of the island than at the open ocean site. Findings of this study are relevant to the aquaculture sector or small scale wave energy developers (e.g. <100 kW), as an insight is provided into the interaction between ocean swell and localised wind seas in semi-sheltered areas.

Keywords: ***Wave Power; Aquaculture; ADCP; Wave buoy; Swell; Wind Sea***

1. Introduction

Wave data analysis for an area east of Colonsay in the Inner Hebrides in Scotland is presented in this paper. The site is currently licensed for an aquaculture development by site operator Marine Harvest (http://www.marineharvest.com/) who was the driving force behind the data acquisition activity, together with wave power developer Albatern (http://albatern.co.uk/) whose interest was in assessing the feasibility of a WEC deployment to provide power to the fish farm cages. The data analysis provides an insight into the relevant differences between the incoming Atlantic swell at the ocean facing site of the area and the sea states observed at the sheltered lee of the island. Applicability of

findings presented here is not limited to this particular site, but is also given to other locations globally with a similar layout. Data is presented from a Datawell Waverider buoy and a Nortek 1MHz AWAC (Acoustic Wave and Current) profiler type at 20 m deployment depth and 1 km distance between devices for a 6 week period in spring 2015, and a comparison with another wave measurement buoy in about 100m depth 100 km to the west of Colonsay is also included.

Following on from the demise of leading wave power developers such as Aquamarine Power, Voith Hydro Wavegen and Pelamis is a realisation that it may not be necessary for early generation wave power projects to target large scale power production at the most energetic sites available (The Crown Estate, 2015). The development of wave energy converter (WEC) technology at sites with a more modest wave exposure is now considered an important interim step towards the development of larger scale projects. One such smaller scale project that has recently secured support from Wave Energy Scotland (WES) is demonstrating additionality by supplying power to an aquaculture site in an area protected from ocean swell and with a modest short period wave climate (Wave Energy Scotland, 2015). Considering the global growth rate of the aquaculture sector including in areas with a good wave resource (e.g. Scotland or Chile), there is an opportunity to utilise wave power on smaller scale (< 100 kW per device) e.g. by replacing on-site diesel-generation on fish farms. The production of potable water through membrane filtration, direct driving of hydraulic systems or pumps (e.g. oil exploration or shore-based aquaculture) or the small scale production of electricity to provide power to island communities are other WEC applications suitable for small to medium power sites (Albatern, 2015; Grey Island Energy Inc., 2015). The economic use of wave energy to power aquaculture sites is dependent on close proximity of WECs to the fish cages, and thus these WEC deployments will be in areas not primarily chosen for their wave resource, but to support the aquaculture activities. Such sites are generally not fully exposed to the ocean swells, but have a limited fetch area resulting in infrequent short crested wind seas, and these may require and/or allow different approaches with view to an optimised energy extraction.

This paper aims to improve the wave resource characterisation process at low to medium energy sites by showing the interaction of swell diffracted around a headland with more localised wind seas. Improved understanding of sea state modifications during the transition from exposed to more sheltered sites informs the design of both WECs and new generation fish cages. It also supports the refinement of operations strategies to allow aquaculture site developments in areas more exposed than what was previously considered suitable. Data and methodologies presented here are relevant to both small scale WEC developers and operators of aquaculture sites.

2. Study Site

A geographical overview of the wider area including the study site off the east coast of Colonsay, part of the Inner Hebrides of Scotland, and additional offshore buoy locations referenced in this paper are shown in Figure 1 with the detailed locational arrangement between the floating wave buoy and the bottom deployed AWAC shown in the inset. Bathymetry at the site is relatively uniform with depth increasing at a shallow gradient towards 40m away from the shore of the island, before it shallows again towards the nearest adjacent islands. The area is exposed to a semidiurnal tidal cycle with a maximum range of around 4 m during spring tides and this is reduced to as little as 1 m during neaps.

Both sensors were deployed in a depth of approximately 20 m chart datum and perpendicular distance to shore was 1.25 km for the buoy and 1.6 km for the AWAC, with a distance of 1 km between both sensors. With the AWAC being deployed slightly further offshore and also closer to the northern end of Colonsay it was expected to capture more of the incoming Atlantic swell, compared with the buoy which was in a slightly more sheltered area. In addition to Colonsay to the east of the study site wave fetch is limited by the islands Islay at 19 km distance to the south, Jura at 13 km to the east and the Isle of Mull at 20 km towards the north. The site is also exposed to a longer fetch area of more than 50 km in a north-easterly direction towards Loch Linnhe and this is of considerable relevance for any installations at the site during the occasionally occurring north-easterly winter storms. The distance to the northern end of Colonsay is less than 4 km and from there to the west the nearest landmasses are Greenland and Canada at some 2,000 km and 3,000 km distance respectively. The wave regime at the west side of the island is predominantly swell based and one of the purposes of this study was to assess the extent to which the Atlantic swell refracts/diffracts towards the east coast of Colonsay.

3. Data Acquisition System

An obvious advantage of deploying multiple sensors capable of measuring similar data is the provided redundancy compared to individual sensor deployments. By combining different types of equipment it is further possible to increase the number of parameters measured and also to identify any potential bias in any one of the returned dual measured parameters. This study presents a comparison between a submerged AWAC and a floating Datawell Waverider buoy. Details of sensors and setup are provided in Table 1.

Previous studies comparing different types of wave measurement devices including those used here have reported that acoustic Doppler current profilers (ADCP) deployed in intermediate depths of 40m appear to be superior in the detection of low period swell during moderate sea states, whilst having a similar ability to detect short period waves, than surface based floating buoys (Bouferrouk et al., 2016). The minimum resolvable wave period for floating buoys is limited by the ratio between buoy diameter and wave length and further impacted by the mooring line and buoy. Attributed to higher

sample rates and improved processing algorithms incorporating data returns from a variety of slanted and vertical acoustic beams, it is suggested that for shallow water deployments ADCPs offer a superior solution to measure both long period swell events, but also multi-directional short crested wind seas of higher frequency than floating bodies (Shih et al., 2005; Shih, 2012; Bendfeld et al., 2008). Although a general conclusion appears to be that ADCPs compare favourably against floating buoys in relatively shallow water, awareness of device and post processing specific features is essential, as comparison between multiple ADCPs operating at different frequencies and using different post processing software for the same deployment location can reveal a bias of one instrument against the other (Hoitink and Schroevers, 2004). Unreliable data returns from floating wave sensors during storm conditions at exposed sites are attributed to data processing response functions following high accelerations in very steep or breaking waves, or in the case of acoustic surface tracking (AST) to insufficient data returns due to a high level of aeration in the water column (Vogler and Venugopal, 2015a; Cahill, 2013). For swell waves under those conditions pressure measurements of an ADCP deployed in shallow water were found to be more reliable than the acoustic backscatter and this strongly supports the approach to parallelise AST measurements with pressure data sampled at a rate sufficient to capture swell waves (Vogler and Venugopal, 2015a). Challenges and information on data acquisition failures encountered during measurements at wave power sites are reported in a review by Lindroth and Leijon (2011).

The buoy deployment commenced in February 2014 and the AWAC was installed in January 2015, driven by Marine Harvest's requirement to gather tidal range and current data. The AWAC was deployed 1.16 km to the north-east of the buoy in a rigid tripod frame mounted on a concrete slab as gravity mooring. This arrangement was chosen as no gimballed tripod was available at the time of the deployment, and was considered suitable based on the shallow gradient of the seafloor at the site and the composition of the seabed. Although the initial values for pitch and roll at the deployment site were with 2° and 0.3° respectively well within boundaries set by the manufacturer, these values changed during gale conditions after 6 weeks to 26° and 34° for pitch and roll and this has resulted in unreliable data returns thereafter. However, for the majority of the initial period between 22/01/2015 to 09/03/2015, i.e. a period of 46 days, good quality data was returned by both buoy and AWAC for supplementary analysis. The AWAC was set up to measure 4,096 samples at 4 Hz frequency with the acoustic beams and 2,048 pressure samples at 2 Hz at the same time for the initial 17 minutes of every half hour and useful data was recorded throughout the initial 46 day deployment. Currents were measured for 24 cells of 1 m each with an initial blanking distance of 0.4 m of the acoustic transducers at the beginning of each wave burst over a 60 s averaging period, and also at 20 minutes and 50 minutes after each full hour. As no live data stream from the AWAC was available the increased pitch and roll was unfortunately only detected on retrieval after the 6 month deployment

period. The wave buoy was providing continuous heave and horizontal displacement data at a 1.28 Hz sample frequency via a live radio link to a shore station.

In addition to the sensors deployed to the east of Colonsay, data was downloaded from the CEFAS Wavenet (CEFAS, 2015) site for the 'Blackstone' buoy, 100 km to the west of Colonsay, and also for the 'West of Hebrides' buoy for a correlation study between the Colonsay data and the incoming Atlantic swell. The locations of these two supplementary buoys, both Datawell Waverider Mk III type and deployed in approximately 100 m depth, relative to the Colonsay site are also indicated on Figure 1.

4. Data Analysis

Datasets from both sensors at Colonsay were processed initially through the proprietary software platforms 'W@ves21' from Datawell for the Waverider Buoy and Nortek 'Storm' for the AWAC. Data quality control was implemented through the supplier's software in the first instance, and this was followed by further statistical and visual analysis of the returned data. Analysis of the data has shown that for the AWAC the signal quality of the AST beam was compromised for 77 data returns out of 2214 records, i.e. 3.5%. In those instances when AST data was compromised wave parameters were processed using the PUV method, in which directional data is derived from the combination of pressure sensor readings and velocity data in x and y directions. For the buoy no data was recorded by the shore based receiver station for 14.5 hours or 1.3% of the same deployment interval, likely caused by power outages. In addition to the raw data outputs both W@ves21 and Nortek Storm also provide statistical and spectral information based on direct time series analysis and Fourier transform of the directional sea surface elevation data. However, no detailed spectral or time-series statistical information is provided from the Nortek Storm software when operating in PUV mode. Only data of a reduced resolution in the frequency domain was available from the CEFAS operated offshore buoys 'Blackstone' and 'West of Hebrides', which was downloaded from the Wavenet online database (CEFAS, 2015) in pre-processed *.csv file format. Although all relevant statistical and spectral parameters could be downloaded from the database, the distribution of the spectral frequency bins was irregular with limited or no information for wind-sea related higher frequencies. For analysis in this study the spectral data from the wave buoys was re-binned at 0.01 Hz intervals for all frequencies to allow a direct comparison with the AWAC dataset. As sufficient data was available for the Colonsay Waverider buoy re-binning was implemented by simple linear interpolation. In case of the Blackstone buoy due to the irregular and limited number of bins publicly available, a spline was fitted across the points using Bessel interpolation to achieve evenly spaced frequency bins corresponding with Colonsay buoy and AWAC. Based on the frequency bin size and power spectral density (PSD) values, spectral moments were calculated as shown in equation (1). Significant wave height H_{m0} and

the energy period (T_E) were then calculated from the zeroth and negative first moments as shown in equations (2) and (3), where reliable spectral data was available.

$$m_n = \sum_j PSD(f_j) \times {f_j}^n \times \Delta f_j \quad (1)$$

$$H_{m0} = 4 \times \sqrt{m_0} \quad (2)$$

$$T_E = \frac{m_{-1}}{m_0} \quad (3)$$

where m_n represents the moment of the nth order, f_j the frequency per bin, Δf_j the spacing of the frequency bins which are equidistant in this case, $PSD(f_j)$ the power spectral density values, and n the order of the moment. In cases where only insufficient spectral data was available, e.g. in some instances for the AWAC when the acoustic signal quality was poor, or for the Blackstone Buoy, where insufficient spectral data points were available to calculate the moments based energy period, a simplified approach was chosen, following Cornett's suggestion (Cornett, 2008) to relate T_E to peak or zero crossing period by multiplying T_p or T_z with either 0.9 or 1.15 respectively. This suggested approach has been tested by Vogler and Venugopal (2015b) for a location west off the Outer Hebrides and was found to be of reasonable accuracy for the peak period, but not so much for the zero crossing period. Therefore the energy period for the Blackstone Buoy location and the AWAC during PUV mode operation was established in this study, based on equation (4).

$$T_E = 0.9 \times T_p \quad (4)$$

For further analysis and comparison of the individual datasets wave power was calculated following linear wave theory by equation (5), where ρ is the density of sea water, taken here as 1,025kgm^{-3}. The group velocity (Cg) used in equation (5) was derived through establishing wavelength (λ), celerity (c), and wave number (k) as shown in equations (6) to (9), where d represents the water depth at the sensor locations.

$$P \approx \rho g \frac{(H_{m0})^2}{16} C_g\,(T_E, d) \quad (5)$$

$$\lambda = \frac{g{T_E}^2}{2\pi} tanh\left(\frac{2\pi d}{\lambda}\right) \quad (6)$$

$$c = \frac{gT_E}{2\pi} \tanh\left(\frac{2\pi d}{\lambda}\right) \quad (7)$$

$$k = \frac{2\pi}{\lambda} \quad (8)$$

$$C_g = 0.5\left(1 + \frac{2kd}{\sinh(2kd)}\right) c \quad (9)$$

The wave direction as obtained from the sensors was corrected from magnetic to true north by subtracting 4.425° to compensate for the magnetic westerly variation, as established from British Admirality Chart Chart 1796: Barra Head to Point of Ardnamurchan.

5. Results

5.1 Tidal Behaviour

During the 46 day observation period three complete spring-neap tidal cycles were covered. The maximum tidal range and current velocity observed during the period were 4.3 m and 0.68 ms^{-1} respectively and the range reduced to around 1 m during neap tides. Tidal currents were found to be generally weak in close vicinity to the area and the highest value observed was 0.682 ms^{-1} at 18 m distance from the seabed during a flood tide and setting into a north-north-easterly direction. The direction of currents was towards the north-east during flood and south to south-west during the ebb cycles. Generally the direction of the current veered constantly in a clockwise direction from ebb to flood, and also further clockwise when changing back to the ebb cycle.

5.2 Wave height

Monthly averaged significant wave height for a one year period from July 2014 – June 2015 is shown in Figure 2 to display the seasonal variation range from 0.19 m only in July to a maximum average value of 0.71 m in January. (Accuracy of buoy measurements has been confirmed during a post deployment calibration check by the supplier). Figure 3 displays the significant wave height H_{m0} for the Colonsay sensors against the CEFAS managed offshore buoy 'Blackstone' and 'West of Hebrides' to the west of South Uist of the Outer Hebrides for the analysis period covered in this paper. The latter buoy was included for comparison against the wave heights observed at the 'Blackstone' location, as these were higher than what was anticipated after an initial review of the Colonsay data. However, wave heights at both locations 'Blackstone' and 'West of Hebrides' compared well, and the system redundancy provided at the Colonsay site through the deployment of multiple sensors also provided high certainty on the lesser wave heights measured there.

It is clearly evident from the wave height plot that the offshore buoys feature a much more energetic wave resource, by more than a factor of 5 for the significant wave height, than the area in the sheltered lee of Colonsay. The general trend for wave height at the Colonsay sensors follows the offshore pattern in some instances but not always. A similarity of the trend is observed when the offshore buoys are exposed to wind driven seas, with the Colonsay sensors being exposed to the same wind regime. In these situations all locations experience a similar increase in wave height as a result of the same weather system passing through the area. But in some other instances there appears to be localised wind near Colonsay only, where the near shore sensors register an increase in wave height

not experienced further offshore – or this increase is too small to be detected and processed in the significant wave height against the background of the much higher ocean swell. In other instances swell from weather systems far away is recorded by the offshore buoys and these swell related wave heights are not or only marginally registered by the near shore sensors.

The distributions of wave heights for the Blackstone location and both Colonsay sensors are plotted in Figures 4(a) and 4(b), together with the best fitted Rayleigh and Weibull distributions, based on the minimum root mean square error (RMS_{error}) and calculated as shown in equation (10), where y represents sample size, x_1 the calculated values and x_2 the empirical data for the distribution data. RMS_{error} values are shown in Table 2. The wave height distribution from the empirical data near Colonsay fit the Rayleigh curve quite well, and this is particularly true for the AWAC data, where the best fitted Weibull curve has returned a shape factor of k = 2 and is thus is identical to the Rayleigh distribution. This is different for the Blackstone location, where a deviation from the Rayleigh distribution is noted for measured wave heights of between 2.5 – 4 m. This is believed to be a result of the short data gathering period, and an extended deployment would likely increase the similarity of measured and fitted distributions.

$$RMS_{error} = \sqrt{\frac{1}{y}\sum(x_1 - x_2)^2} \tag{10}$$

As an alternative to the Weibull and Rayleigh distributions plotted in Figures 4(a) and 4(b), an attempt was made to fit the data with the Kernel Density estimator, expressed by equation (11)

$$f_h(x) = \frac{1}{yh}\sum_{i=1}^{y} K\left(\frac{x - x_i}{h}\right); \qquad -\infty < x < \infty \tag{11}$$

where x_i is the sample (i.e., wave height), y is the sample size, h is the bandwidth and $K(\bullet)$ is the Kernel function. The results are shown in Figures 5(a) to 5(c) for Blackstone, Colonsay buoy and AWAC respectively. The values of bandwidth, mean, median and standard deviations obtained for each site are tabulated in Table 3. It is evident from Figures 5(a) to 5(c) that, the bimodality in the measured wave height is better fitted by the Kernel density function than with the Weibull and Rayleigh models, hence the Kernel density function might be an acceptable alternative to describe the wave data considered here for analysis. Further, the standard deviation (std) values of the wave height calculated from measured data at Blackstone, Colonsay wave buoy and Colonsay AWAC are 2.08 m, 0.29 m and 0.31 m respectively, which are very close to the std values reported in Table 3 using the Kernel density function.

5.3 Wave Period

The data shows a clear correlation between wave height and period, and this is particularly evident for the offshore location. For approximately one third of the observations the area in the lee of Colonsay has shown short crested wind seas of less than 6 s peak period. The remaining observations of the same area displayed typical behaviour of swell waves with peak periods of more than 10 s and up to 20 s. Very few records were returned of between 6 – 10 s and a step change was visible from short period wind seas to longer period swell waves. At times dominated by swell waves the area east of Colonsay showed very similar values to those measured further offshore and this shows the progression of swell around the island to the sheltered lee. The Blackstone buoy data has returned peak period values indicating a dominant swell regime almost throughout, and only on a limited number of occasions the period fell below 10 s, and never below 5 s. A histogram showing the distribution of the peak period for the 2182 half hourly observed data intervals is shown in Figure 6. Good similarity with a Rayleigh distribution is shown for the Blackstone data series for peak periods of > 9 s. The distributions for AWAC and Colonsay Buoy are more complex due to the bimodal nature of the period distribution, and the absence of observed wave periods between 5 s and 10 s. From the directional distribution of the peak period shown in Figure 7 it is evident that the longer period swell waves east of Colonsay are entirely approaching from the north-east with any dominant seas from the south being of a shorter local wind sea related period. This bimodal distribution of wave periods seen in Figures 6 and 7 for the Colonsay sites cannot be modelled by the Rayleigh distribution alone, and an approach similar to the one taken for significant wave heights above was followed by applying a Kernel density estimation to the Peak wave periods for all three sites with results being shown in Figures 8(a) to 8 (c). The corresponding statistical parameters are presented in Table 4. The Kernel density method appears to fit the wave period data very well. As already observed for the wave heights, a comparison of standard deviation values from measured data with the ones estimated from the Kernel density fitting also shows good correlation for the wave period for the three locations. (Values are 2.55 s, 4.98 s and 4.44 s for Blackstone, Colonsay wave buoy and AWAC respectively). The two distinct groups of wave periods observed for Colonsay buoy and AWAC are clearly represented by the Kernel density functions, demonstrating its suitability as a density estimator for situations where wave propagation is governed by swell and local wind sea.

The clear distinction between wind sea and swell components as visible in the peak period for the Colonsay sensors disappears when considering the distribution of the zero up-crossing period (T_z) shown in Figure 9. For T_z both the Colonsay buoy and AWAC are of a much narrower bandwidth than the offshore buoy, which is scattered over more than 6 s, compared against a range of only 4 s for the sensors at the more sheltered location. The AWAC has registered a higher number of waves with a zero crossing period of less than 3 s than the Colonsay buoy, and this may be because of the higher sampling rate of 4 Hz compared against the 1.28Hz sample frequency of the buoy. Another

explanation could be due to site character as the wave buoy was situated in a slightly more sheltered location than the AWAC.

5.4 Directional Spread

A histogram of the directional spread of waves for the Colonsay sensors and the 'Blackstone' buoy is shown in Figure 10. The peak directional spread of a unimodal sea state is defined as the spread of the incoming waves at the most energetic frequency. In situations with bimodality and incoming waves of similar power density from multiple directions, the spread is defined as the angular distance between the individual peaks (Datawell, 2012). Dominated by the Atlantic swell the 'Blackstone' buoy shows a considerable smaller directional spread with a peak occurrence and average value of around 30°. The directional spread at this location ranges primarily between 25° to 45°, with a small number of outliers of up to 79° on isolated timestamps, when no single dominant direction was prevalent. The directional spread is much higher at the Colonsay Buoy and AWAC location for most of the time with average values of 39° and 48° respectively. It is not fully clear why a higher spread has been registered at the AWAC location, which is somewhat more exposed to the incoming swell than the Colonsay buoy. A likely explanation is in the higher bimodality experienced between diffracted and refracted swell coming from the north-east and already deprived of most of its power density due to diffraction, refraction and shoaling, and wind seas from a predominant west to south-westerly direction. Due to the energy losses experienced by the swell, the magnitude of both wind seas and swell in those circumstances may be similar and thus both are registered by the software as a bimodal wave regime with an angular spread of up to 80° between the diffracted swell and wind sea from the south. As the Colonsay buoy is situated a little further south and thus more sheltered from the swell, less bimodality is experienced and the shown spread is more attributable to the wind generated seas only. This is supported by a comparison of the power spectral density at the swell related frequency bands, where the AWAC shows a higher energy content than the AWAC. The difference in spread between the nearshore sensors may further be explained by differences in post processing of the data between the Datawell and Nortek software solutions.

5.5 Wave Power

Following the calculation of wavelength and group velocity the wave power for the three sensor locations was calculated as shown in equation (5) and is plotted in Figure 11. For better scalability the offshore power is displayed as $100kWm^{-1}$ wave crest, against the Colonsay data which follows the standard convention of units as kWm^{-1}. Although due to the exposed nature of the Blackstone location wave power was expected to be much higher compared against the lee of Colonsay, the difference of almost two orders of magnitude is more than what was anticipated. The wave power at the AWAC and Colonsay buoy locations follows the trend of the offshore buoy and most of the swell based energy appears still to be registered at the lee of the island, albeit at a much reduced level. But

in addition on a number of occasions the AWAC and Colonsay buoy are also exposed to some isolated increases of power which were not observed at the offshore location, and these are likely related to some localised wind driven sea states in the area. The average power over the 46 day simultaneous deployment during winter 2015 was 167 kWm^{-1} at the Blackstone Buoy location and 2.36 kWm^{-1} and 1.46 kWm^{-1} at the Colonsay AWAC and buoy respectively. The average values for H_{m0}, T_z and wave power for the observation period are summarised in Table 5.

5.6 Percentage occurrences of wave height and direction

The directional distribution of significant wave height is shown as the percentage of occurrences in Figures 12, 13, and 14 for Blackstone, AWAC and Colonsay Buoy locations respectively. The predominant westerly wave direction at Blackstone with the majority of wave heights between 4 to 7 m changes in the lee of Colonsay to a northerly to north-easterly direction at the AWAC, with a further clockwise change of direction towards the buoy location. The dominant direction observed at the AWAC is with 15 to 25° about 40° less than what was measured by the wave buoy. This additional directional shift, caused by diffraction and refraction, also translates into a reduction of wave height with the majority of waves observed by the buoy from that direction of 0.5 to 1 m, compared with a higher amount of northerly sea states of 1 to 1.5 m registered by the AWAC. Of interest is the amount of wind seas of around 0.5 to 1 m from the southerly direction measured by both Colonsay buoy and AWAC. This amounts for approximately 20% of observed sea states and creates a clear bi-directionality which must be considered when planning any development in the area. As the direction shown in Figures 12 to 14 only relates to the peak energy, the site will also quite often be exposed to a bi-modal sea state with swell waves from a north-easterly direction interacting with wind seas from the south and thus causing a confused sea state. It can be expected that an analysis of the sea states in the lee of the south of Colonsay will show that the directional shifts through processes of diffraction and refraction act in a counter clockwise direction here, thus aligning the incoming swell with the wind seas, and this is relevant to resource assessment for energy extraction or aquaculture development. A full analysis of the directional spectra, together with a numerical model of the wider domain can provide more information on this, is currently in development, but is not part of this paper.

5.7 Frequency distribution of Energy Density

The bimodality observed for the peak period of the sensors sheltered from the main swell is also evident when looking at the time averaged frequency distribution of the power spectral density (PSD) shown in Figure 15. (It should be noted that the line representing the Blackstone buoy is divided by 100 to allow scalability against the other plots which are of considerable less energy). Where the Blackstone buoy has a clearly defined single peak at about 0.075 Hz, this peak is also well developed for the AWAC and Colonsay buoy locations. However, for the latter two sensors, there also is a

secondary peak of a broader nature between 0.225 to 0.25 Hz and this corresponds to the wind seas of around 4 s period shown in Figure 6. Considering that the significant wave height is related to the zeroth moment of the power density spectrum as shown in equation (2), the wave power equation (5) can be rearranged and be related to m_0 as shown in equation (12).

$$P \approx \rho g m_0 C_g\,(fe, d) \tag{12}$$

As m_0 is represented by the area under the PSD curves (e.g. in Figure 15), it is clearly indicated that the energy available from the higher period sea states around the 0.25 Hz frequency band is of a comparable significance in the lee of the island to that of the longer period swell wave dominated sea states. The weekly PSD averages for the AWAC location are shown in Figure 16 to show the variability of sea states. Over the six week observation period a difference of around an order of magnitude between the sea states with the lowest and highest amount of energy was observed at all sites, where the lowest energy was encountered in the week starting 01 February, and the highest values being returned at the beginning of March. But during all sea states throughout the measurement campaign bimodality was observed on the PSD frequency distribution by both AWAC and Colonsay buoy.

6. Discussion

In nearshore and coastal region, as sea levels can vary dramatically due to tides, storm surges, and wind generated waves and swells, the application of a particular probability distribution or probability density function (pdf) to represent the short- and long-term wave conditions needs verification. A pdf provides an understanding of the changes in sea water levels and wave periods, particularly in extreme events such as storms and hurricanes, and is highly critical to the successful design of any ocean structure, including aquaculture systems or wave energy converters as in this case. With a successful wave height probability distribution method, the expected water levels over the life time of a structure can be determined and several wave parameters can also be estimated. The Rayleigh distribution (Longuet-Higgins (1980)), which works well for narrow banded Gaussian ocean waves, and the Weibull distribution are popular models used in describing wave heights. For shallow water, Battjes and Groenendijk (2000) suggested a combination of Rayleigh distribution for low wave heights and of Weibull type for high wave heights. For a combined wind-swell seas (bimodal seas), it appears that no probability distribution model exists. Rodriguez et al., (2002) inspected this through numerical simulation of sea states and calculated probability distributions using Rayleigh, Weibull, Naess (1985), Vinje (1989), and Tayfun (1990) models, and concluded that none of these models were able to adequately predict the exceedance probabilities in bimodal sea states. In the absence of reliable model to fit swell-wind waves, for the present work, a Kernel density based distribution

(Equation 11) was used in this paper in addition to Rayleigh and Weibull, and their relative predictive accuracy has been shown.

Findings of this study are relevant to potential users of the area for a number of reasons. The site is targeted for an aquaculture development and as such regular access to the individual fish cages is required throughout the year. Information as presented in this study can inform the design and choice of craft to be used to ensure safe access and transit to and from this and similar sites. In addition to the planned aquaculture development, consideration is given to the installation of a small size WEC system to reduce the requirement of diesel generation on the fish farm. The site is not dissimilar from other sites targeted for this type of developments and thus information presented in this paper on the diffraction of swell into the lee of an island and its interaction with localised wind seas is applicable to other areas with a similar geographical layout and development opportunities.

A comprehensive understanding of the different sea states encountered at potential WEC deployment sites is relevant to safe operation and to inform energy yield, reliability and survivability. Related to these aspects the bimodality of the observed wave periods and direction, and the complex sea state resulting from the interaction of both, is of particular interest.

Although sheltered against extreme wave heights during storm events, the associated periods are still detectable, if not predominant, thus creating a bimodal sea state due to the combination of local wind seas and swell. A close understanding of these longer swell wave related periods is an important design factor for the avoidance of natural frequencies of aquaculture structures, such as feed barges or fish cages, that are often moored at such sites for considerable lengths of time.

In the context of WEC performance operation at natural frequencies is desirable to maximise yield. Considering that the performance of many WEC systems is related to the ratio between mass, device geometry and wavelength, an understanding of the wave periods and bi-directionality within a sea state is crucial for the assessment of device design and performance. For most WECs the performance is greatly reduced during operations outwith a narrow frequency band. It should be considered whether performance analysis is best based on the entire measured frequency spectrum, or if an improved approach would introduce a limitation of the analysis to a narrower frequency band covering WEC specific design frequencies only. For example, Figure 15 shows a peak frequency at the 0.075 Hz mark, with a secondary peak of lesser magnitude near 0.225 Hz. A WEC for deployment in such sheltered locations may well be tuned to target shorter wavelengths as associated with the secondary peak, thus maximising energy production from wind seas rather than ocean swell. Using default spectral processing based on peak period, or energy period, the optimal conditions for a specific WEC at a given site could easily be missed, as a secondary peak at the perfect frequency would not be singled out. Also the significant wave height obtained over the full measured frequency band will differ from an H_{m0} value calculated for a narrow frequency band only, resulting in

misleading yield assessments for specific WECs. A better approach may be to limit the frequency range to work out spectral parameters to those frequencies that are useful for energy production only, thus improving the accuracy of energy production forecasting. A possible solution to this problem could be to establish two different values for e.g. the significant wave height, one for the entire measured frequency spectrum, i.e. a standard H_{m0}, and a secondary value $H_{m0[fa-fb]}$, where the subscript [fa-fb] defines the useful frequency band, for the energy producing part of the spectrum. Here it is suggested that future (publicly funded) resource assessment studies follow this approach to produce data for multiple frequency bands, as this will be of greater use for WEC developers than the current approach where only the entire frequency spectrum is considered. In a context where private sector funding is difficult to obtain for WEC development, and production of detailed resource assessments is the obligation of developers, it would help desk based preliminary site assessments if this detail was added to numerical resource maps to not add to the financial burden of a struggling sector.

Although the energy available at sheltered sites as investigated here may be too small to consider large scale production and export scenarios of electricity, there is a considerable local market with remote communities, or aquaculture developments that only require smaller amount of electricity. With an average wave power in the lee of Colonsay over the study period of 1.46 kWm^{-1}, and based on the extend of the island of approximately 15 km from south-west to north-east, the total amount of energy available is around 1.46 kWm^{-1} x 15 km = 21.9 MW. Based on an approximate total of 70 households and an assumed average power usage of 2 kW per house, the total electrical average power requirement is only 140 kW, i.e. is covered by only 100 m of wave front on average, or 320 m when considering an efficiency of 30 %. The expertise and knowledge gained from the operations of small scale wave energy systems in sheltered locations as presented here could be an important stepping stone in the advancement of the wave power sector to larger scale.

7. Concluding remarks

Some of the characteristic features of sea conditions in the lee of a Scottish island, Colonsay, are illustrated in this paper using wave data measurements made by a wave buoy and an AWAC. The analysis indicates that the significant wave height at the measurement site is reduced by more than a factor of five times the offshore wave height within a space of about 100 km. In an attempt to fit the wave heights and wave periods by Rayleigh, Weibull and Kernel density distributions, it appears that Kernel density approach fits the data well. It is found that the swell components do not progress into the lee of the island due to reduction of wave heights, nevertheless, the peak periods corresponding to swell remains unchanged at the more sheltered location. It is suggested that the bimodality as can be found in the combination of swell waves and wind seas at the study site requires careful consideration when assessing the suitability of a site for WEC deployment, and it is proposed to consider the exclusion of those parts of the frequency spectrum that are not contributing to energy production of a

WEC, by incorporating only relevant frequencies in the yield related spectral analysis. It is shown that even a relatively modest energy resource as presented in this study may have the potential to provide sufficient power to island communities and other small scale end users. To this end the development of such sites for WEC deployment may well be an important stepping stone in the progression of the wave energy sector to maturity at larger scale.

Although the estimated wave power at the study site is small when compared against a nearby offshore location, there may still be opportunities to develop such a modest wave power resource in the context of small scale community power or fish farming. Devices such as Albatern's Squid, Eco Wave Power's Wave clapper device (Maritime Journal, 2016), or of the ReBaS Generator type (Vogler et al., 2016) designed to operate at rated output at less energetic sites than open ocean facing areas, could possibly achieve high efficiencies when deployed at the Colonsay study site, or sites with a similar character. A numerical model to investigate the bimodality of wave direction and period along the entire lee coast of Colonsay is currently in development. Such a model will allow identification of the optimum device specific site for WEC installations by matching the bimodal WEC response against a micro scale resource assessment.

Acknowledgements

The authors would like to acknowledge MERIKA (FP7/2007-2013 Grant agreement 315925), Marine Harvest, Albatern, and Hebrides Marine Services Ltd as funders and partners of this study. Furthermore thanks are also expressed to the CEFAS Wavenet for providing wave data for the Blackstone and West of Hebrides site.

References

Albatern Wave Energy, 2015. Markets. http://albatern.co.uk/markets/ (accessed 30/12/2015).

Bendfeld, J. et al., 2008. ADCP and Waverider Measurements for O&M at offshore wind farm locations. In: European Wind Energy Conference & Exhibition (EWEC 2008), Bruxelles, Belgium.

Bouferrouk, A. et al., 2016. Field measurements of surface waves using a 5-beamADCP. Ocean Engineering, 112 (2016), pp. 173-184.

Cahill, B., 2013. Characteristics of the wave energy resource at the Atlantic marine energy test site. PhD Thesis, University College Cork.

CEFAS, 2015. WaveNet interactive map. http://wavenet.cefas.co.uk/Map (accessed on 27/12/2015).

Cornett, A.M., 2008. A Global wave energy resource assessment. In: Proceedings of the 18th (2008) International Offshore and Polar Engineering Conference, Vancouver, BC, Canada, July 6-11, vol.1, pp. 318-326.

Datawell BV, 2012. DWR MkIII and DWR4 – A comparative report on the DWRIII and DWR4 data. Haarlem: Datawell BV, T.30.01, p.11.

Datawell BV, 2014. Datawell Waverider Reference Manual DWR-MkIII DWR-G. Heerhugowaard: Datawell BV Oceanographic Instruments, p. 38.

Grey Island Energy Inc., 2015. Applications. http://www.greyislandenergy.com/#!applications/c17q0 (accessed 30/12/2015).

Hoitink, A.J.F. and Schroevers, M., 2004. Validation of ADCP surface wave measurements in a shelf sea. In: OCEANS '04. MTTS/IEEE Techno-Ocean '04, Kobe, November 2004, IEEE, vol.3, no., pp.1444-1451 Vol.3.

Lindroth, S., Leijon, M., 2011. Offshore wave power measurements – A review. Renewable and Sustainable Energy Reviews, 15 (2011), pp. 4274 – 4285.

Maritime Journal, 2016. Eco Wave Power completes installation of innovative device in Gibraltar. http://www.maritimejournal.com/news101/marine-renewable-energy/eco-wave-power-completes-installation-of-innovative-device-in-gibraltar (accessed 04/06/2016).

Nortek AS, 2002. Wave Measurements using the PUV method. Rud, Norway: Nortek AS, 2002/Doc.No. N4000-720.

Nortek AS, 2005. AWAC Acoustic Wave and Current Meter User Guide. Rud, Norway: Nortek AS, Doc. No: N3000-126 Revision E 09.2005.

Shih, H. H. et al., 2005. Intercomparison of Wave Data Between Triaxys Directional Wave Buoy, ADCP, and Other Reference Wave Instruments. In: Proceedings of the ASME2005 24th International Conference on Offshore Mechanics and Arctic Engineering: Volume 2, Halkidiki, Greece, 12-17 June 2005, pp. 655-663.

Longuet-Higgins, M. S. 1980. On the Distribution of the Heights of Sea Waves: Some Effects of Nonlinearity and Finite Bandwidth, Journal of Geophysical Research, Vol 85, pp 1519-1523.

Battjes, J.A., and H.W. Groenendijk, 2000. Wave height distributions on shallow foreshores, Coastal Engineering, Vol. 40, pp 161-182.

Rodriguez, G. R., and Guedes Soares, C., Mercedes, Pe´rez-Martell, E. 2002. Wave Height Distribution in Mixed Sea States. ASME J. Offshore Mech. Arct. Eng., 124, 2002. pp. 34–40.

Naess, A., 1985. On the Statistical Distribution of Crest to Trough Wave Heights, Ocean Eng., 12, 221–234.

Vinje, T., 1989. The Statistical Distribution of Wave Heights in a Random Seaway,'' Appl. Ocean. Res., 119, 143–152.

Tayfun, A., 1990, Distribution of Large Wave Heights, J. Wtrway., Port, Coast., and Oc. Eng., 116, 686–707.

Shih, H.H., 2012. Real-time current and wave measurements in ports and harbors using ADCP. In: OCEANS, 2012 - Yeosu, IEEE, May 2012, pp.1-8.

The Crown Estate, 2015. New leasing for small scale wave and tidal sites. http://www.thecrownestate.co.uk/news-and-media/news/2015/new-leasing-for-small-scale-wave-and-tidal-sites/ (accessed 02/08/2016).

Vogler, A. and Venugopal, V., 2015a. Wave Sensor Observations during a severe Storm event at a Marine Energy Development Site. In: Proceedings of the 11th European Wave and Tidal Energy Conference (EWTEC 2015), September 2015. Nantes.

Vogler, A. and Venugopal, V., 2015b. Observations on Shallow Water Wave Distributions at an Ocean Energy Site. In: Proceedings of the ASME 2015 34th International Conference on Ocean, Offshore and Arctic Engineering. Volume 7: Ocean Engineering, St. John's, Newfoundland, May 31–June 5, 2015, pp. V007T06A063.

Vogler, A. et al., 2016. Performance of a point pivoted WEC equipped with a linear ball screw generator in regular wave conditions. In: Proceedings of CORE 2016 2nd International Conference on Offshore Renewable Energy. Glasgow, 12 – 14 September 2016.

Wave Energy Scotland, 2015. Wave energy first for Scottish aquaculture. http://www.hie.co.uk/growth-sectors/energy/wave-energy-scotland/news-and-events/news/wave-energy-first-for-scottish-aquaculture.html (accessed 06/06/2016).

Wave data analysis for a semi-sheltered site in the Inner Hebrides of Scotland suitable for small scale WEC development

Authors:

1. Arne Vogler, Marine Energy Research Group, Lews Castle College, University of the Highlands and Islands, Stornoway, Isle of Lewis, Scotland, GB-HS2 0XR, arne.vogler@uhi.ac.uk

2. Vengatesan Venugopal, School of Engineering, The University of Edinburgh, Faraday Building, King's Buildings, Colin Maclaurin Road, Edinburgh, UK, EH9 3DW, V.Venugopal@ed.ac.uk

Corresponding author: Arne Vogler, +44(0)1851 770 325, e-mail: arne.vogler@uhi.ac.uk

Abstract

Wave data analysis from a short-term deployment of a wave buoy and AWAC in the lee of a Hebridean island in the United Kingdom is discussed in this paper. Significant parameters are calculated and Rayleigh, Weibull and Kernel density probability distributions have been employed to fit the measured data. Results show that while the Atlantic facing side of the island is exposed to a predominant swell based wave regime, the area in the lee features bimodality for wave period and directionality. The Kernel density distribution is found to fit the measured bimodality well compared to Rayleigh and Weibull distributions. The analysis illustrates that interference between swell waves and associated wave periods from north with southerly wind driven seas creates a complex sea state. It is shown that the higher wind sea related frequency components are of more significance in the lee of the island than at the open ocean site. ~~This is useful knowledge to develop and tune wave energy converters (WEC) to an optimised level.~~ Findings of this study are relevant to the aquaculture sector or small scale wave energy developers (e.g. <100 kW), as an insight is provided into the interaction between ocean swell and localised wind seas in semi-sheltered areas.

Keywords: ***Wave Power; Aquaculture; ADCP; Wave buoy; Swell; Wind Sea***

1. Introduction

Wave data analysis for an area east of Colonsay in the Inner Hebrides in Scotland is presented in this paper. The site is currently licensed for an aquaculture development by site operator Marine Harvest (http://www.marineharvest.com/) who was the driving force behind the data acquisition activity, together with wave power developer Albatern (http://albatern.co.uk/) whose interest was in assessing

the feasibility of a WEC deployment to provide power to the fish farm cages. The data analysis provides an insight into the relevant differences between the incoming Atlantic swell at the ocean facing site of the area and the sea states observed at the sheltered lee of the island. Applicability of findings presented here is not limited to this particular site, but is also given to other locations globally with a similar layout. Data is presented from a Datawell Waverider buoy and a Nortek 1MHz AWAC (Acoustic Wave and Current) profiler type at 20 m deployment depth and 1 km distance between devices for a 6 week period in spring 2015, and a comparison with another wave measurement buoy in about 100m depth 100 km to the west of Colonsay is also included.

Following on from the demise of leading wave power developers such as Aquamarine Power, Voith Hydro Wavegen and Pelamis is a realisation that it may not be necessary for early generation wave power projects to target large scale power production at the most energetic sites available (The Crown Estate, 2015). The development of wave energy converter (WEC) technology at sites with a more modest wave exposure is now considered an important interim step towards the development of larger scale projects. One such smaller scale project that has recently secured support from Wave Energy Scotland (WES) is demonstrating additionality by supplying power to an aquaculture site in an area protected from ocean swell and with a modest short period wave climate (Wave Energy Scotland, 2015). Considering the global growth rate of the aquaculture sector including in areas with a good wave resource (e.g. Scotland or Chile), there is an opportunity to utilise wave power on smaller scale (< 100 kW per device) ~~small scale wave power~~ e.g. by replacing on-site diesel-generation on fish farms. The production of potable water through membrane filtration, direct driving of hydraulic systems or pumps (e.g. oil exploration or shore-based aquaculture) or the small scale production of electricity to provide power to island communities are other WEC applications suitable for small to medium power sites (Albatern, 2015; Grey Island Energy Inc., 2015). The economic use of wave energy to power aquaculture sites is dependent on close proximity of WECs to the fish cages, and thus these WEC deployments will be in areas not primarily chosen for their wave resource, but to support the aquaculture activities. Such sites are generally not fully exposed to the ocean swells, but have a limited fetch area resulting in infrequent short crested wind seas, and these may require and/or allow different approaches with view to an optimised energy extraction.

This paper aims to improve the wave resource characterisation process at low to medium energy sites by showing the interaction of swell diffracted around a headland with more localised wind seas. Improved understanding of sea state modifications during the transition from exposed to more sheltered sites informs the design of both WECs and new generation fish cages. It also supports the refinement of operations strategies to allow aquaculture site developments in areas more exposed than what was previously considered suitable. Data and methodologies presented here are relevant to both small scale WEC developers and operators of aquaculture sites.

2. Study Site

A geographical overview of the wider area including the study site off the east coast of Colonsay, part of the Inner Hebrides of Scotland, and additional offshore buoy locations referenced in this paper are shown in Figure 1 with the detailed locational arrangement between the floating wave buoy and the bottom deployed AWAC shown in the inset. Bathymetry at the site is relatively uniform with depth increasing at a shallow gradient towards 40m away from the shore of the island, before it shallows again towards the nearest adjacent islands. The area is exposed to a semidiurnal tidal cycle with a maximum range of around 4 m during spring tides and this is reduced to as little as 1 m during neaps.

Both sensors were deployed in a depth of approximately 20m chart datum and perpendicular distance to shore was 1.25 km for the buoy and 1.6 km for the AWAC, with a distance of 1 km between both sensors. With the AWAC being deployed slightly further offshore and also closer to the northern end of Colonsay it was expected to capture more of the incoming Atlantic swell, compared with the buoy which was in a slightly more sheltered area. In addition to Colonsay to the east of the study site wave fetch is limited by the islands Islay at 19 km distance to the south, Jura at 13 km to the east and the Isle of Mull at 20 km towards the north. The site is also exposed to a longer fetch area of more than 50 km in a north-easterly direction towards Loch Linnhe and this is of considerable relevance for any installations at the site during the occasionally occurring north-easterly winter storms. The distance to the northern end of Colonsay is less than 4 km and from there to the west the nearest landmasses are Greenland and Canada at some 2,000 km and 3,000 km distance respectively. The wave regime at the west side of the island is predominantly swell based and one of the purposes of this study was to assess the extent to which the Atlantic swell refracts/diffracts towards the east coast of Colonsay.

3. Data Acquisition System

An obvious advantage of deploying multiple sensors capable of measuring similar data is the provided redundancy compared to individual sensor deployments. By combining different types of equipment it is further possible to increase the number of parameters measured and also to identify any potential bias in any one of the returned dual measured parameters. This study presents a comparison between a submerged AWAC and a floating Datawell Waverider buoy. Details of sensors and setup are provided in Table 1.

Previous studies comparing different types of wave measurement devices including those used here have reported that acoustic Doppler current profilers (ADCP) deployed in intermediate depths of 40m appear to be superior in the detection of low period swell during moderate sea states, whilst having a

similar ability to detect short period waves, than surface based floating buoys (Bouferrouk et al., 2016). The minimum resolvable wave period for floating buoys is limited by the ratio between buoy diameter and wave length and further impacted by the mooring line and buoy. Attributed to higher sample rates and improved processing algorithms incorporating data returns from a variety of slanted and vertical acoustic beams, it is suggested that for shallow water deployments ADCPs offer a superior solution to measure both long period swell events, but also multi-directional short crested wind seas of higher frequency than floating bodies (Shih et al., 2005; Shih, 2012; Bendfeld et al., 2008). Although a general conclusion appears to be that ADCPs compare favourably against floating buoys in relatively shallow water, awareness of device and post processing specific features is essential, as comparison between multiple ADCPs operating at different frequencies and using different post processing software for the same deployment location can reveal a bias of one instrument against the other (Hoitink and Schroevers, 2004). Unreliable data returns from floating wave sensors during storm conditions at exposed sites are attributed to data processing response functions following high accelerations in very steep or breaking waves, or in the case of acoustic surface tracking (AST) to insufficient data returns due to a high level of aeration in the water column (Vogler and Venugopal, 2015a; Cahill, 2013). For swell waves under those conditions pressure measurements of an ADCP deployed in shallow water were found to be more reliable than the acoustic backscatter and this strongly supports the approach to parallelise AST measurements with pressure data sampled at a rate sufficient to capture swell waves (Vogler and Venugopal, 2015a). Challenges and information on data acquisition failures encountered during measurements at wave power sites are reported in a review by Lindroth and Leijon (2011).

The buoy deployment commenced in February 2014 and the AWAC was installed in January 2015, driven by Marine Harvest's requirement to gather tidal range and current data. The AWAC was deployed 1.16 km to the north-east of the buoy in a rigid tripod frame mounted on a concrete slab as gravity mooring. This arrangement was chosen as no gimballed tripod was available at the time of the deployment, and was considered suitable based on the shallow gradient of the seafloor at the site and the composition of the seabed. Although the initial values for pitch and roll at the deployment site were with 2° and 0.3° respectively well within boundaries set by the manufacturer, these values changed during gale conditions after 6 weeks to 26° and 34° for pitch and roll and this has resulted in unreliable data returns thereafter. However, for the majority of the initial period between 22/01/2015 to 09/03/2015, i.e. a period of 46 days, good quality data was returned by both buoy and AWAC for supplementary analysis. The AWAC was set up to measure 4,096 samples at 4 Hz frequency with the acoustic beams and 2,048 pressure samples at 2 Hz at the same time for the initial 17 minutes of every half hour and useful data was recorded throughout the initial 46 day deployment. Currents were measured for 24 cells of 1 m each with an initial blanking distance of 0.4 m of the acoustic transducers at the beginning of each wave burst over a 60 s averaging period, and also at 20 minutes

and 50 minutes after each full hour. As no live data stream from the AWAC was available the increased pitch and roll was unfortunately only detected on retrieval after the 6 month deployment period. The wave buoy was providing continuous heave and horizontal displacement data at a 1.28 Hz sample frequency via a live radio link to a shore station.

In addition to the sensors deployed to the east of Colonsay, data was downloaded from the CEFAS Wavenet (CEFAS, 2015) site for the 'Blackstone' buoy, 100 km to the west of Colonsay, and also for the 'West of Hebrides' buoy for a correlation study between the Colonsay data and the incoming Atlantic swell. The locations of these two supplementary buoys, both Datawell Waverider Mk III type and deployed in approximately 100 m depth, relative to the Colonsay site are also indicated on Figure 1.

4. Data Analysis

Datasets from both sensors at Colonsay were processed initially through the proprietary software platforms 'W@ves21' from Datawell for the Waverider Buoy and Nortek 'Storm' for the AWAC. Data quality control was implemented through the supplier's software in the first instance, and this was followed by further statistical and visual analysis of the returned data. Analysis of the data has shown that for the AWAC the signal quality of the AST beam was compromised for 77 data returns out of 2214 records, i.e. 3.5%. In those instances when AST data was compromised wave parameters were processed using the PUV method, in which directional data is derived from the combination of pressure sensor readings and velocity data in x and y directions. For the buoy no data was recorded by the shore based receiver station for 14.5 hours or 1.3% of the same deployment interval, likely caused by power outages. In addition to the raw data outputs both W@ves21 and Nortek Storm also provide statistical and spectral information based on direct time series analysis and Fourier transform of the directional sea surface elevation data. However, no detailed spectral or time-series statistical information is provided from the Nortek Storm software when operating in PUV mode. Only data of a reduced resolution in the frequency domain was available from the CEFAS operated offshore buoys 'Blackstone' and 'West of Hebrides', which was downloaded from the Wavenet online database (CEFAS, 2015) in pre-processed *.csv file format. Although all relevant statistical and spectral parameters could be downloaded from the database, the distribution of the spectral frequency bins was irregular with limited or no information for wind-sea related higher frequencies. For analysis in this study the spectral data from the wave buoys was re-binned at 0.01 Hz intervals for all frequencies to allow a direct comparison with the AWAC dataset. As sufficient data was available for the Colonsay Waverider buoy re-binning was implemented by simple linear interpolation. In case of the Blackstone buoy due to the irregular and limited number of bins publicly available, a spline was fitted across the points using Bessel interpolation to achieve evenly spaced frequency bins corresponding with Colonsay buoy and AWAC. Based on the frequency bin size and power spectral density (PSD)

values, spectral moments were calculated as shown in equation (1). Significant wave height H_{m0} and the energy period (T_E) were then calculated from the zeroth and negative first moments as shown in equations (2) and (3), where reliable spectral data was available.

$$m_n = \sum_j PSD(f_j) \times {f_j}^n \times \Delta f_j \quad (1)$$

$$H_{m0} = 4 \times \sqrt{m_0} \quad (2)$$

$$T_E = \frac{m_{-1}}{m_0} \quad (3)$$

where m_n represents the moment of the nth order, f_j the frequency per bin, Δf_j the spacing of the frequency bins which are equidistant in this case, $PSD(f_j)$ the power spectral density values, and n the order of the moment. In cases where only insufficient spectral data was available, e.g. in some instances for the AWAC when the acoustic signal quality was poor, or for the Blackstone Buoy, where insufficient spectral data points were available to calculate the moments based energy period, a simplified approach was chosen, following Cornett's suggestion (Cornett, 2008) to relate T_E to peak or zero crossing period by multiplying T_p or T_z with either 0.9 or 1.15 respectively. This suggested approach has been tested by Vogler and Venugopal (2015b) for a location west off the Outer Hebrides and was found to be of reasonable accuracy for the peak period, but not so much for the zero crossing period. Therefore the energy period for the Blackstone Buoy location and the AWAC during PUV mode operation was established in this study, based on equation (4).

$$T_E = 0.9 \times T_p \quad (4)$$

For further analysis and comparison of the individual datasets wave power was calculated following linear wave theory by equation (5), where ρ is the density of sea water, taken here as 1,025kgm^{-3}. The group velocity (Cg) used in equation (5) was derived through establishing wavelength (λ), celerity (c), and wave number (k) as shown in equations (6) to (9), where d represents the water depth at the sensor locations.

$$P \approx \rho g \frac{(H_{m0})^2}{16} C_g\,(T_E, d) \quad (5)$$

$$\lambda = \frac{g{T_E}^2}{2\pi} tanh\left(\frac{2\pi d}{\lambda}\right) \quad (6)$$

$$c = \frac{gT_E}{2\pi} \tanh\left(\frac{2\pi d}{\lambda}\right) \quad (7)$$

$$k = \frac{2\pi}{\lambda} \quad (8)$$

$$C_g = 0.5\left(1 + \frac{2kd}{\sinh(2kd)}\right) c \quad (9)$$

The wave direction as obtained from the sensors was corrected from magnetic to true north by subtracting 4.425° to compensate for the magnetic westerly variation, as established from British Admirality Chart Chart 1796: Barra Head to Point of Ardnamurchan.

5. Results

5.1 Tidal Behaviour

During the 46 day observation period three complete spring-neap tidal cycles were covered. The maximum tidal range and current velocity observed during the period were 4.3 m and 0.68 ms^{-1} respectively and the range reduced to around 1 m during neap tides. Tidal currents were found to be generally weak in close vicinity to the area and the highest value observed was 0.682 ms^{-1} at 18 m distance from the seabed during a flood tide and setting into a north-north-easterly direction. The direction of currents was towards the north-east during flood and south to south-west during the ebb cycles. Generally the direction of the current veered constantly in a clockwise direction from ebb to flood, and also further clockwise when changing back to the ebb cycle..

5.2 Wave height

Monthly averaged significant wave height for a one year period from July 2014 – June 2015 is shown in Figure 2 to display the seasonal variation range from 0.19 m only in July to a maximum average value of 0.71 m in January. (Accuracy of buoy measurements has been confirmed during a post deployment calibration check by the supplier). Figure 3 displays the significant wave height H_{m0} for the Colonsay sensors against the CEFAS managed offshore buoy 'Blackstone' and 'West of Hebrides' to the west of South Uist of the Outer Hebrides for the analysis period covered in this paper. The latter buoy was included for comparison against the wave heights observed at the 'Blackstone' location, as these were higher than what was anticipated after an initial review of the Colonsay data. However, wave heights at both locations 'Blackstone' and 'West of Hebrides' compared well, and the system redundancy provided at the Colonsay site through the deployment of multiple sensors also provided high certainty on the lesser wave heights measured there.

It is clearly evident from the wave height plot that the offshore buoys feature a much more energetic wave resource, by more than a factor of 5 for the significant wave height, than the area in the sheltered lee of Colonsay. The general trend for wave height at the Colonsay sensors follows the offshore pattern in some instances but not always. A similarity of the trend is observed when the offshore buoys are exposed to wind driven seas, with the Colonsay sensors being exposed to the same wind regime. In these situations all locations experience a similar increase in wave height as a result of the same weather system passing through the area. But in some other instances there appears to be localised wind near Colonsay only, where the near shore sensors register an increase in wave height

not experienced further offshore – or this increase is too small to be detected and processed in the significant wave height against the background of the much higher ocean swell. In other instances swell from weather systems far away is recorded by the offshore buoys and these swell related wave heights are not or only marginally registered by the near shore sensors.

The distributions of wave heights for the Blackstone location and both Colonsay sensors are plotted in Figures 4(a) and 4(b), together with the best fitted Rayleigh and Weibull distributions, based on the minimum root mean square error (RMS_{error}) and calculated as shown in equation (10), where y represents sample size, x_1 the calculated values and x_2 the empirical data for the distribution data. RMS_{error} values are shown in Table 2. The wave height distribution from the empirical data near Colonsay fit the Rayleigh curve quite well, and this is particularly true for the AWAC data, where the best fitted Weibull curve has returned a shape factor of k = 2 and is thus is identical to the Rayleigh distribution. This is different for the Blackstone location, where a deviation from the Rayleigh distribution is noted for measured wave heights of between 2.5 – 4 m. This is believed to be a result of the short data gathering period, and an extended deployment would likely increase the similarity of measured and fitted distributions.

$$RMS_{error} = \sqrt{\frac{1}{y}\sum(x_1 - x_2)^2} \tag{10}$$

As an alternative to the Weibull and Rayleigh distributions plotted in Figures 4(a) and 4(b), an attempt was made to fit the data with the Kernel Density estimator, expressed by equation (11)

$$f_h(x) = \frac{1}{yh}\sum_{i=1}^{y} K\left(\frac{x - x_i}{h}\right); \qquad -\infty < x < \infty \tag{11}$$

where x_i is the sample (i.e., wave height), y is the sample size, h is the bandwidth and $K(\bullet)$ is the Kernel function. The results are shown in Figures 5(a) to 5(c) for Blackstone, Colonsay buoy and AWAC respectively. The values of bandwidth, mean, median and standard deviations obtained for each site are tabulated in Table 3. It is evident from Figures 5(a) to 5(c) that, the bimodality in the measured wave height is better fitted by the Kernel density function than with the Weibull and Rayleigh models, hence the Kernel density function might be an acceptable alternative to describe the wave data considered here for analysis. Further, the standard deviation (std) values of the wave height calculated from measured data at Blackstone, Colonsay wave buoy and Colonsay AWAC are 2.08 m, 0.29 m and 0.31 m respectively, which are very close to the std values reported in Table 3 using the Kernel density function.

5.3 Wave Period

The data shows a clear correlation between wave height and period, and this is particularly evident for the offshore location. For approximately one third of the observations the area in the lee of Colonsay has shown short crested wind seas of less than 6 s peak period. The remaining observations of the same area displayed typical behaviour of swell waves with peak periods of more than 10 s and up to 20 s. Very few records were returned of between 6 – 10 s and a step change was visible from short period wind seas to longer period swell waves. At times dominated by swell waves the area east of Colonsay showed very similar values to those measured further offshore and this shows the progression of swell around the island to the sheltered lee. The Blackstone buoy data has returned peak period values indicating a dominant swell regime almost throughout, and only on a limited number of occasions the period fell below 10 s, and never below 5 s. A histogram showing the distribution of the peak period for the 2182 half hourly observed data intervals is shown in Figure 6. Good similarity with a Rayleigh distribution is shown for the Blackstone data series for peak periods of > 9 s. The distributions for AWAC and Colonsay Buoy are more complex due to the bimodal nature of the period distribution, and the absence of observed wave periods between 5 s and 10 s. From the directional distribution of the peak period shown in Figure 7 it is evident that the longer period swell waves east of Colonsay are entirely approaching from the north-east with any dominant seas from the south being of a shorter local wind sea related period. This bimodal distribution of wave periods seen in Figures 6 and 7 for the Colonsay sites cannot be modelled by the Rayleigh distribution alone, and an approach similar to the one taken for significant wave heights above was followed by applying a Kernel density estimation to the Peak wave periods for all three sites with results being shown in Figures 8(a) to 8 (c). The corresponding statistical parameters are presented in Table 4. The Kernel density method appears to fit the wave period data very well. As already observed for the wave heights, a comparison of standard deviation values from measured data with the ones estimated from the Kernel density fitting also shows good correlation for the wave period for the three locations. (Values are 2.55 s, 4.98 s and 4.44 s for Blackstone, Colonsay wave buoy and AWAC respectively). The two distinct groups of wave periods observed for Colonsay buoy and AWAC are clearly represented by the Kernel density functions, demonstrating its suitability as a density estimator for situations where wave propagation is governed by swell and local wind sea.

The clear distinction between wind sea and swell components as visible in the peak period for the Colonsay sensors disappears when considering the distribution of the zero up-crossing period (T_z) shown in Figure 9. For T_z both the Colonsay buoy and AWAC are of a much narrower bandwidth than the offshore buoy, which is scattered over more than 6 s, compared against a range of only 4 s for the sensors at the more sheltered location. The AWAC has registered a higher number of waves with a zero crossing period of less than 3 s than the Colonsay buoy, and this may be because of the higher sampling rate of 4 Hz compared against the 1.28Hz sample frequency of the buoy. Another

explanation could be due to site character as the wave buoy was situated in a slightly more sheltered location than the AWAC.

5.4 Directional Spread

A histogram of the directional spread of waves for the Colonsay sensors and the 'Blackstone' buoy is shown in Figure 10. The peak directional spread of a unimodal sea state is defined as the spread of the incoming waves at the most energetic frequency. In situations with bimodality and incoming waves of similar power density from multiple directions, the spread is defined as the angular distance between the individual peaks (Datawell, 2012). Dominated by the Atlantic swell the 'Blackstone' buoy shows a considerable smaller directional spread with a peak occurrence and average value of around 30°. The directional spread at this location ranges primarily between 25° to 45°, with a small number of outliers of up to 79° on isolated timestamps, when no single dominant direction was prevalent. The directional spread is much higher at the Colonsay Buoy and AWAC location for most of the time with average values of 39° and 48° respectively. It is not fully clear why a higher spread has been registered at the AWAC location, which is somewhat more exposed to the incoming swell than the Colonsay buoy. A likely explanation is in the higher bimodality experienced between diffracted and refracted swell coming from the north-east and already deprived of most of its power density due to diffraction, refraction and shoaling, and wind seas from a predominant west to south-westerly direction. Due to the energy losses experienced by the swell, the magnitude of both wind seas and swell in those circumstances may be similar and thus both are registered by the software as a bimodal wave regime with an angular spread of up to 80° between the diffracted swell and wind sea from the south. As the Colonsay buoy is situated a little further south and thus more sheltered from the swell, less bimodality is experienced and the shown spread is more attributable to the wind generated seas only. This is supported by a comparison of the power spectral density at the swell related frequency bands, where the AWAC shows a higher energy content than the AWAC. The difference in spread between the nearshore sensors may further be explained by differences in post processing of the data between the Datawell and Nortek software solutions.

5.5 Wave Power

Following the calculation of wavelength and group velocity the wave power for the three sensor locations was calculated as shown in equation (5) and is plotted in Figure 11. For better scalability the offshore power is displayed as $100kWm^{-1}$ wave crest, against the Colonsay data which follows the standard convention of units as kWm^{-1}. Although due to the exposed nature of the Blackstone location wave power was expected to be much higher compared against the lee of Colonsay, the difference of almost two orders of magnitude is more than what was anticipated. The wave power at the AWAC and Colonsay buoy locations follows the trend of the offshore buoy and most of the swell based energy appears still to be registered at the lee of the island, albeit at a much reduced level. But

in addition on a number of occasions the AWAC and Colonsay buoy are also exposed to some isolated increases of power which were not observed at the offshore location, and these are likely related to some localised wind driven sea states in the area. The average power over the 46 day simultaneous deployment during winter 2015 was 167 kWm^{-1} at the Blackstone Buoy location and 2.36 kWm^{-1} and 1.46 kWm^{-1} at the Colonsay AWAC and buoy respectively. The average values for H_{m0}, T_z and wave power for the observation period are summarised in Table 5.

5.6 Percentage occurrences of wave height and direction

The directional distribution of significant wave height is shown as the percentage of occurrences in Figures 12, 13, and 14 for Blackstone, AWAC and Colonsay Buoy locations respectively. The predominant westerly wave direction at Blackstone with the majority of wave heights between 4 to 7 m changes in the lee of Colonsay to a northerly to north-easterly direction at the AWAC, with a further clockwise change of direction towards the buoy location. The dominant direction observed at the AWAC is with 15 to 25° about 40° less than what was measured by the wave buoy. This additional directional shift, caused by diffraction and refraction, also translates into a reduction of wave height with the majority of waves observed by the buoy from that direction of 0.5 to 1 m, compared with a higher amount of northerly sea states of 1 to 1.5 m registered by the AWAC. Of interest is the amount of wind seas of around 0.5 to 1 m from the southerly direction measured by both Colonsay buoy and AWAC. This amounts for approximately 20% of observed sea states and creates a clear bi-directionality which must be considered when planning any development in the area. As the direction shown in Figures 12 to 14 only relates to the peak energy, the site will also quite often be exposed to a bi-modal sea state with swell waves from a north-easterly direction interacting with wind seas from the south and thus causing a confused sea state. It can be expected that an analysis of the sea states in the lee of the south of Colonsay will show that the directional shifts through processes of diffraction and refraction act in a counter clockwise direction here, thus aligning the incoming swell with the wind seas, and this is relevant to resource assessment for energy extraction or aquaculture development. A full analysis of the directional spectra, together with a numerical model of the wider domain can provide more information on this, is currently in development, but is not part of this paper.

5.7 Frequency distribution of Energy Density

The bimodality observed for the peak period of the sensors sheltered from the main swell is also evident when looking at the time averaged frequency distribution of the power spectral density (PSD) shown in Figure 15. (It should be noted that the line representing the Blackstone buoy is divided by 100 to allow scalability against the other plots which are of considerable less energy). Where the Blackstone buoy has a clearly defined single peak at about 0.075 Hz, this peak is also well developed for the AWAC and Colonsay buoy locations. However, for the latter two sensors, there also is a

secondary peak of a broader nature between 0.225 to 0.25 Hz and this corresponds to the wind seas of around 4 s period shown in Figure 6. Considering that the significant wave height is related to the zeroth moment of the power density spectrum as shown in equation (2), the wave power equation (5) can be rearranged and be related to m_0 as shown in equation (12).

$$P \approx \rho g m_0 C_g\,(fe, d) \tag{12}$$

As m_0 is represented by the area under the PSD curves (e.g. in Figure 15), it is clearly indicated that the energy available from the higher period sea states around the 0.25 Hz frequency band is of a comparable significance in the lee of the island to that of the longer period swell wave dominated sea states. The weekly PSD averages for the AWAC location are shown in Figure 16 to show the variability of sea states. Over the six week observation period a difference of around an order of magnitude between the sea states with the lowest and highest amount of energy was observed at all sites, where the lowest energy was encountered in the week starting 01 February, and the highest values being returned at the beginning of March. But during all sea states throughout the measurement campaign bimodality was observed on the PSD frequency distribution by both AWAC and Colonsay buoy.

6. Discussion

In nearshore and coastal region, as sea levels can vary dramatically due to tides, storm surges, and wind generated waves and swells, the application of a particular probability distribution or probability density function (pdf) to represent the short- and long-term wave conditions needs verification. A pdf provides an understanding of the changes in sea water levels and wave periods, particularly in extreme events such as storms and hurricanes, and is highly critical to the successful design of any ocean structure, including aquaculture systems or wave energy converters as in this case. With a successful wave height probability distribution method, the expected water levels over the life time of a structure can be determined and several wave parameters can also be estimated. The Rayleigh distribution (Longuet-Higgins (1980)), which works well for narrow banded Gaussian ocean waves, and the Weibull distribution are popular models used in describing wave heights. For shallow water, Battjes and Groenendijk (2000) suggested a combination of Rayleigh distribution for low wave heights and of Weibull type for high wave heights. For a combined wind-swell seas (bimodal seas), it appears that no probability distribution model exists. Rodriguez et al., (2002) inspected this through numerical simulation of sea states and calculated probability distributions using Rayleigh, Weibull, Naess (1985), Vinje (1989), and Tayfun (1990) models, and concluded that none of these models were able to adequately predict the exceedance probabilities in bimodal sea states. In the absence of reliable model to fit swell-wind waves, for the present work, a Kernel density based distribution

(Equation 11) was used in this paper in addition to Rayleigh and Weibull, and their relative predictive accuracy has been shown.

Findings of this study are relevant to potential users of the area for a number of reasons. The site is targeted for an aquaculture development and as such regular access to the individual fish cages is required throughout the year. Information as presented in this study can inform the design and choice of craft to be used to ensure safe access and transit to and from this and similar sites. In addition to the planned aquaculture development, consideration is given to the installation of a small size WEC system to reduce the requirement of diesel generation on the fish farm. The site is not dissimilar from other sites targeted for this type of developments and thus information presented in this paper on the diffraction of swell into the lee of an island and its interaction with localised wind seas is applicable to other areas with a similar geographical layout and development opportunities.

A comprehensive understanding of the different sea states encountered at potential WEC deployment sites is relevant to safe operation and to inform energy yield, reliability and survivability. Related to these aspects the bimodality of the observed wave periods and direction, and the complex sea state resulting from the interaction of both, is of particular interest.

Although sheltered against extreme wave heights during storm events, the associated periods are still detectable, if not predominant, thus creating a bimodal sea state due to the combination of local wind seas and swell. A close understanding of these longer swell wave related periods is an important design factor for the avoidance of natural frequencies of aquaculture structures, such as feed barges or fish cages, that are often moored at such sites for considerable lengths of time.

In the context of WEC performance operation at natural frequencies is desirable to maximise yield. Considering that the performance of many WEC systems is related to the ratio between mass, device geometry and wavelength, an understanding of the wave periods and bi-directionality within a sea state is crucial for the assessment of device design and performance. For most WECs the performance is greatly reduced during operations outwith a narrow frequency band. It should be considered whether performance analysis is best based on the entire measured frequency spectrum, or if an improved approach would introduce a limitation of the analysis to a narrower frequency band covering WEC specific design frequencies only. For example, Figure 15 shows a peak frequency at the 0.075 Hz mark, with a secondary peak of lesser magnitude near 0.225 Hz. A WEC for deployment in such sheltered locations may well be tuned to target shorter wavelengths as associated with the secondary peak, thus maximising energy production from wind seas rather than ocean swell. Using default spectral processing based on peak period, or energy period, the optimal conditions for a specific WEC at a given site could easily be missed, as a secondary peak at the perfect frequency would not be singled out. Also the significant wave height obtained over the full measured frequency band will differ from an H_{m0} value calculated for a narrow frequency band only, resulting in

misleading yield assessments for specific WECs. A better approach may be to limit the frequency range to work out spectral parameters to those frequencies that are useful for energy production only, thus improving the accuracy of energy production forecasting. A possible solution to this problem could be to establish two different values for e.g. the significant wave height, one for the entire measured frequency spectrum, i.e. a standard H_{m0}, and a secondary value $H_{m0[fa-fb]}$, where the subscript [fa-fb] defines the useful frequency band, for the energy producing part of the spectrum. Here it is suggested that future (publicly funded) resource assessment studies follow this approach to produce data for multiple frequency bands, as this will be of greater use for WEC developers than the current approach where only the entire frequency spectrum is considered. In a context where private sector funding is difficult to obtain for WEC development, and production of detailed resource assessments is the obligation of developers, it would help desk based preliminary site assessments if this detail was added to numerical resource maps to not add to the financial burden of a struggling sector.

Although the energy available at sheltered sites as investigated here may be too small to consider large scale production and export scenarios of electricity, there is a considerable local market with remote communities, or aquaculture developments that only require smaller amount of electricity. With an average wave power in the lee of Colonsay over the study period of 1.46 kWm^{-1}, and based on the extend of the island of approximately 15 km from south-west to north-east, the total amount of energy available is around 1.46 kWm^{-1} x 15 km = 21.9 MW. Based on an approximate total of 70 households and an assumed average power usage of 2 kW per house, the total electrical average power requirement is only 140 kW, i.e. is covered by only 100 m of wave front on average, or 320 m when considering an efficiency of 30 %. The expertise and knowledge gained from the operations of small scale wave energy systems in sheltered locations as presented here could be an important stepping stone in the advancement of the wave power sector to larger scale.

7. Concluding remarks

Some of the characteristic features of sea conditions in the lee of a Scottish island, Colonsay, are illustrated in this paper using wave data measurements made by a wave buoy and an AWAC. The analysis indicates that the significant wave height at the measurement site is reduced by more than a factor of five times the offshore wave height within a space of about 100 km. In an attempt to fit the wave heights and wave periods by Rayleigh, Weibull and Kernel density distributions, it appears that Kernel density approach fits the data well. It is found that the swell components do not progress into the lee of the island due to reduction of wave heights, nevertheless, the peak periods corresponding to swell remains unchanged at the more sheltered location. It is suggested that the bimodality as can be found in the combination of swell waves and wind seas at the study site requires careful consideration when assessing the suitability of a site for WEC deployment, and it is proposed to consider the exclusion of those parts of the frequency spectrum that are not contributing to energy production of a

WEC, by incorporating only relevant frequencies in the yield related spectral analysis. It is shown that even a relatively modest energy resource as presented in this study may have the potential to provide sufficient power to island communities and other small scale end users. To this end the development of such sites for WEC deployment may well be an important stepping stone in the progression of the wave energy sector to maturity at larger scale.

Although the estimated wave power at the study site is small when compared against a nearby offshore location, there may still be opportunities to develop such a modest wave power resource in the context of small scale community power or fish farming. Devices such as Albatern's Squid, Eco Wave Power's Wave clapper device (Maritime Journal, 2016), or of the ReBaS Generator type (Vogler et al., 2016) designed to operate at rated output at less energetic sites than open ocean facing areas, could possibly achieve high efficiencies when deployed at the Colonsay study site, or sites with a similar character. A numerical model to investigate the bimodality of wave direction and period along the entire lee coast of Colonsay is currently in development. Such a model will allow identification of the optimum device specific site for WEC installations by matching the bimodal WEC response against a micro scale resource assessment.

Acknowledgements

The authors would like to acknowledge MERIKA (FP7/2007-2013 Grant agreement 315925), Marine Harvest, Albatern, and Hebrides Marine Services Ltd as funders and partners of this study. Furthermore thanks are also expressed to the CEFAS Wavenet for providing wave data for the Blackstone and West of Hebrides site.

References

Albatern Wave Energy, 2015. Markets. http://albatern.co.uk/markets/ (accessed 30/12/2015).

Bendfeld, J. et al., 2008. ADCP and Waverider Measurements for O&M at offshore wind farm locations. In: European Wind Energy Conference & Exhibition (EWEC 2008), Bruxelles, Belgium.

Bouferrouk, A. et al., 2016. Field measurements of surface waves using a 5-beamADCP. Ocean Engineering, 112 (2016), pp. 173-184.

Cahill, B., 2013. Characteristics of the wave energy resource at the Atlantic marine energy test site. PhD Thesis, University College Cork.

CEFAS, 2015. WaveNet interactive map. http://wavenet.cefas.co.uk/Map (accessed on 27/12/2015).

Cornett, A.M., 2008. A Global wave energy resource assessment. In: Proceedings of the 18th (2008) International Offshore and Polar Engineering Conference, Vancouver, BC, Canada, July 6-11, vol.1, pp. 318-326.

Datawell BV, 2012. DWR MkIII and DWR4 – A comparative report on the DWRIII and DWR4 data. Haarlem: Datawell BV, T.30.01, p.11.

Datawell BV, 2014. Datawell Waverider Reference Manual DWR-MkIII DWR-G. Heerhugowaard: Datawell BV Oceanographic Instruments, p. 38.

Grey Island Energy Inc., 2015. Applications. http://www.greyislandenergy.com/#!applications/c17q0 (accessed 30/12/2015).

Hoitink, A.J.F. and Schroevers, M., 2004. Validation of ADCP surface wave measurements in a shelf sea. In: OCEANS '04. MTTS/IEEE Techno-Ocean '04, Kobe, November 2004, IEEE, vol.3, no., pp.1444-1451 Vol.3.

Lindroth, S., Leijon, M., 2011. Offshore wave power measurements – A review. Renewable and Sustainable Energy Reviews, 15 (2011), pp. 4274 – 4285.

Maritime Journal, 2016. Eco Wave Power completes installation of innovative device in Gibraltar. http://www.maritimejournal.com/news101/marine-renewable-energy/eco-wave-power-completes-installation-of-innovative-device-in-gibraltar (accessed 04/06/2016).

Nortek AS, 2002. Wave Measurements using the PUV method. Rud, Norway: Nortek AS, 2002/Doc.No. N4000-720.

Nortek AS, 2005. AWAC Acoustic Wave and Current Meter User Guide. Rud, Norway: Nortek AS, Doc. No: N3000-126 Revision E 09.2005.

Shih, H. H. et al., 2005. Intercomparison of Wave Data Between Triaxys Directional Wave Buoy, ADCP, and Other Reference Wave Instruments. In: Proceedings of the ASME2005 24th International Conference on Offshore Mechanics and Arctic Engineering: Volume 2, Halkidiki, Greece, 12-17 June 2005, pp. 655-663.

Longuet-Higgins, M. S. 1980. On the Distribution of the Heights of Sea Waves: Some Effects of Nonlinearity and Finite Bandwidth, Journal of Geophysical Research, Vol 85, pp 1519-1523.

Battjes, J.A., and H.W. Groenendijk, 2000. Wave height distributions on shallow foreshores, Coastal Engineering, Vol. 40, pp 161-182.

Rodriguez, G. R., and Guedes Soares, C., Mercedes, Pe´rez-Martell, E. 2002. Wave Height Distribution in Mixed Sea States. ASME J. Offshore Mech. Arct. Eng., 124, 2002. pp. 34–40.

Naess, A., 1985. On the Statistical Distribution of Crest to Trough Wave Heights, Ocean Eng., 12, 221–234.

Vinje, T., 1989. The Statistical Distribution of Wave Heights in a Random Seaway,'' Appl. Ocean. Res., 119, 143–152.

Tayfun, A., 1990, Distribution of Large Wave Heights, J. Wtrway., Port, Coast., and Oc. Eng., 116, 686–707.

Shih, H.H., 2012. Real-time current and wave measurements in ports and harbors using ADCP. In: OCEANS, 2012 - Yeosu, IEEE, May 2012, pp.1-8.

The Crown Estate, 2015. New leasing for small scale wave and tidal sites. http://www.thecrownestate.co.uk/news-and-media/news/2015/new-leasing-for-small-scale-wave-and-tidal-sites/ (accessed 02/08/2016).

Vogler, A. and Venugopal, V., 2015a. Wave Sensor Observations during a severe Storm event at a Marine Energy Development Site. In: Proceedings of the 11th European Wave and Tidal Energy Conference (EWTEC 2015), September 2015. Nantes.

Vogler, A. and Venugopal, V., 2015b. Observations on Shallow Water Wave Distributions at an Ocean Energy Site. In: Proceedings of the ASME 2015 34th International Conference on Ocean, Offshore and Arctic Engineering. Volume 7: Ocean Engineering, St. John's, Newfoundland, May 31–June 5, 2015, pp. V007T06A063.

Vogler, A. et al., 2016. Performance of a point pivoted WEC equipped with a linear ball screw generator in regular wave conditions. In: Proceedings of CORE 2016 2nd International Conference on Offshore Renewable Energy. Glasgow, 12 – 14 September 2016.

Wave Energy Scotland, 2015. Wave energy first for Scottish aquaculture. http://www.hie.co.uk/growth-sectors/energy/wave-energy-scotland/news-and-events/news/wave-energy-first-for-scottish-aquaculture.html (accessed 06/06/2016).

List of Figures

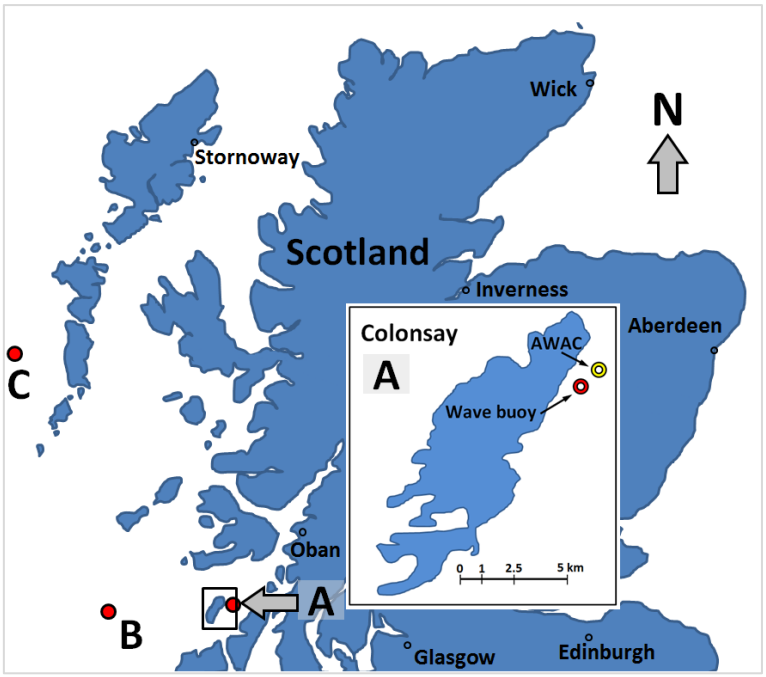

Figure 1 – Geographical Overview. The study site east off Colonsay (detailed map shown in inset) and offshore buoys Blackstone and West of Hebrides are marked A, B and C respectively. Wave buoy co-ordinates are 56° 5.72'N 006° 7.93'W and the distance between Buoy and AWAC is 1.16 km.

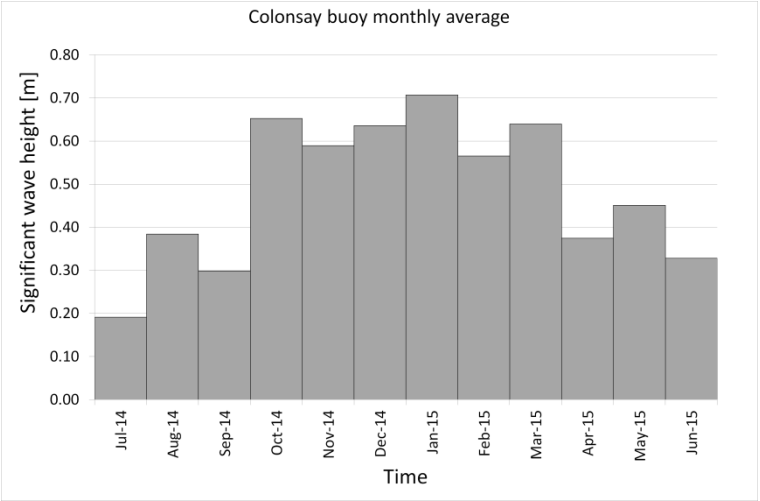

Figure 2 – Monthly averaged significant wave height for one year (Colonsay buoy, Jul 14 – Jun 15)

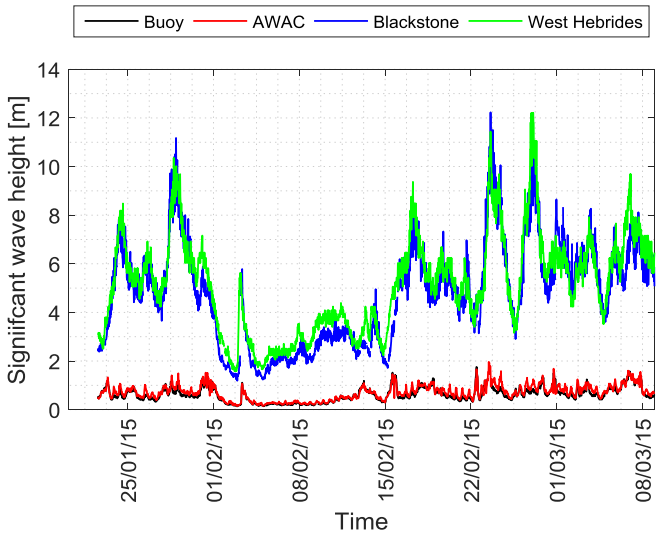

Figure 3 – Significant Wave Height time series offshore buoy and Colonsay sensors

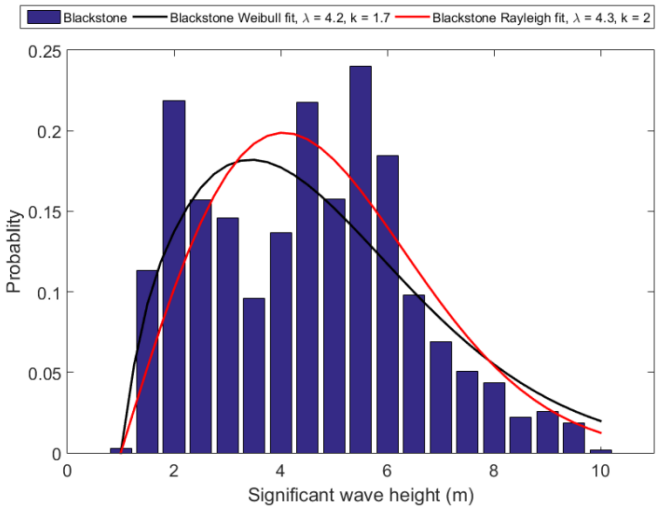

Figure 4(a) – Significant Wave Height distribution at Blackstone

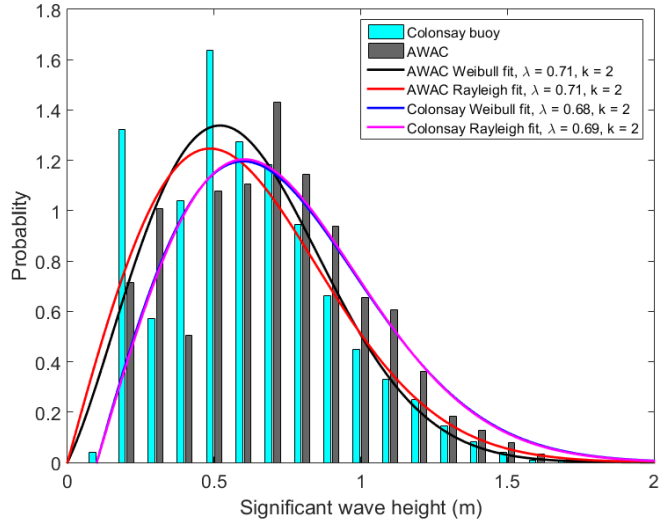

Figure 4(b) – Significant Wave Height distribution at Colonsay

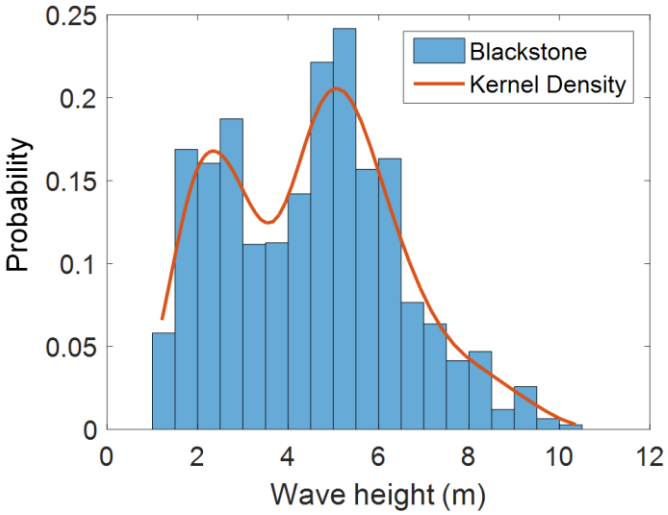

Figure 5(a) – Significant Wave Height distribution at Blackstone with Kernel density estimation

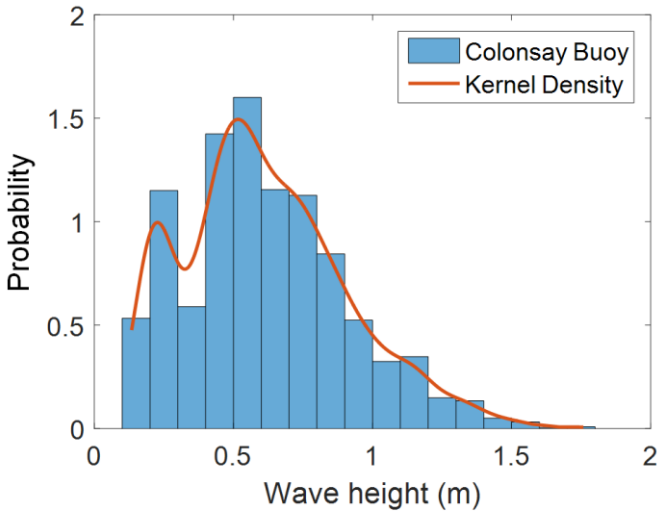

Figure 5(b) – Significant Wave Height distribution at Colonsay wave buoy with Kernel density estimation

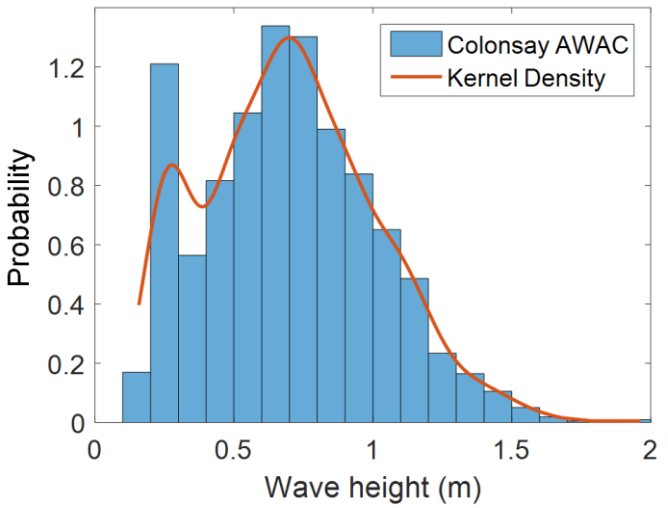

Figure 5(c) – Significant Wave Height distribution at Colonsay AWAC with Kernel density estimation

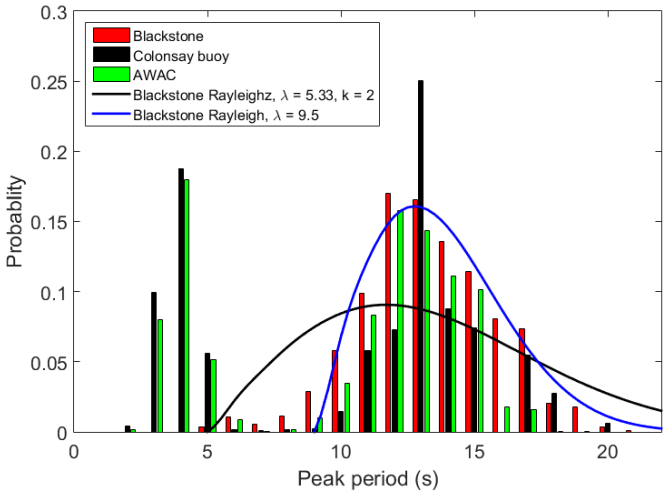

Figure 6 – Distribution of Peak Period

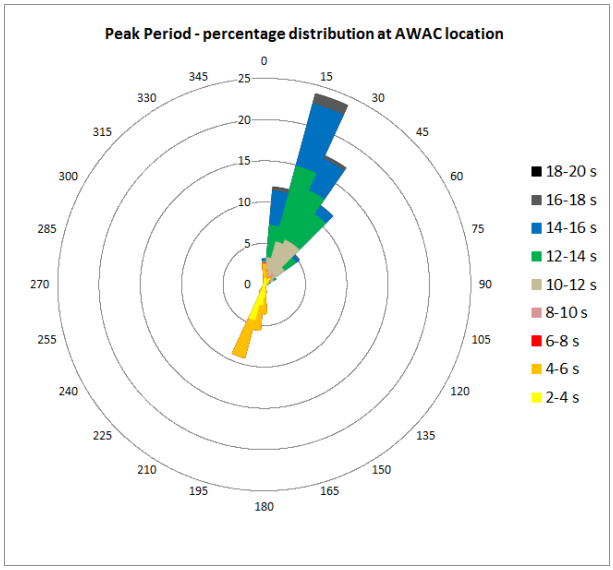

Figure 7 – Directional distribution of peak period in percentage for AWAC location

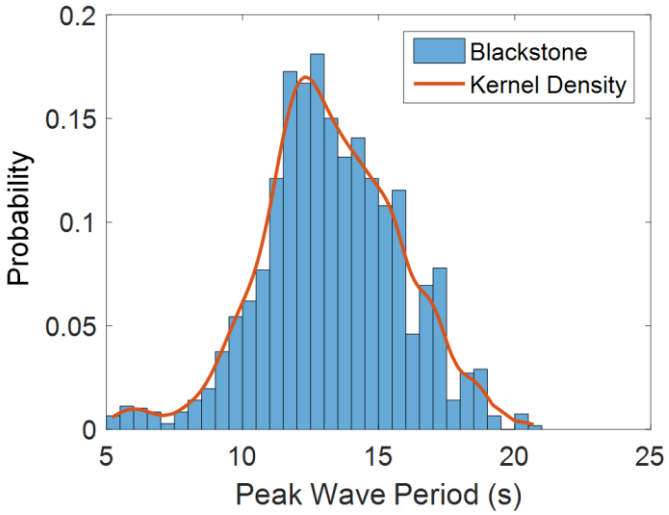

Figure 8(a) – Distribution of Peak Period for Blackstone with Kernel Density estimation

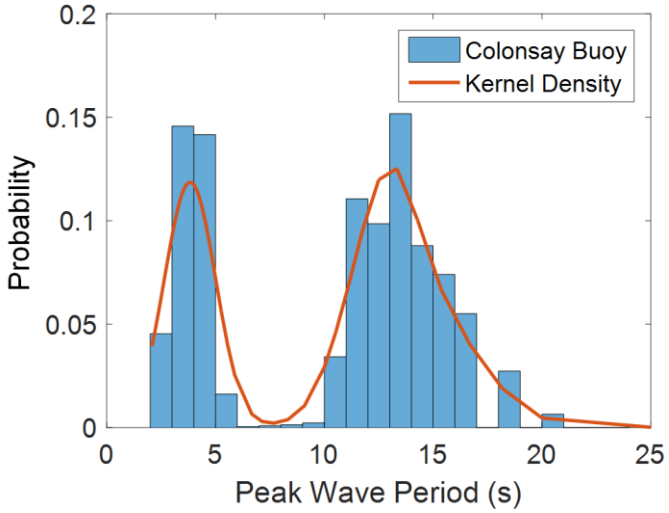

Figure 8(b) – Distribution of Peak Period for Colonsay Buoy with Kernel Density estimation

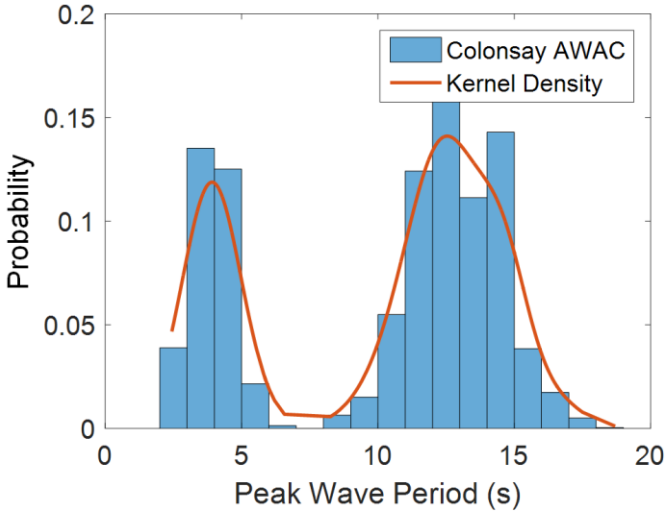

Figure 8(c) – Distribution of Peak Period for Colonsay AWAC with Kernel Density estimation

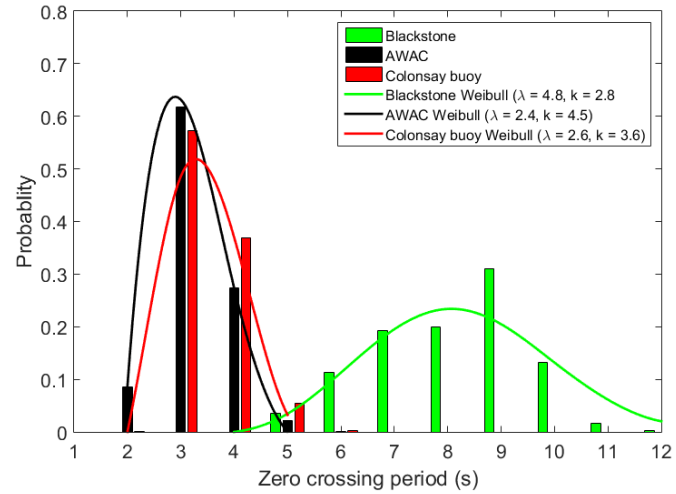

Figure 9 – Distribution of zero up-crossing period

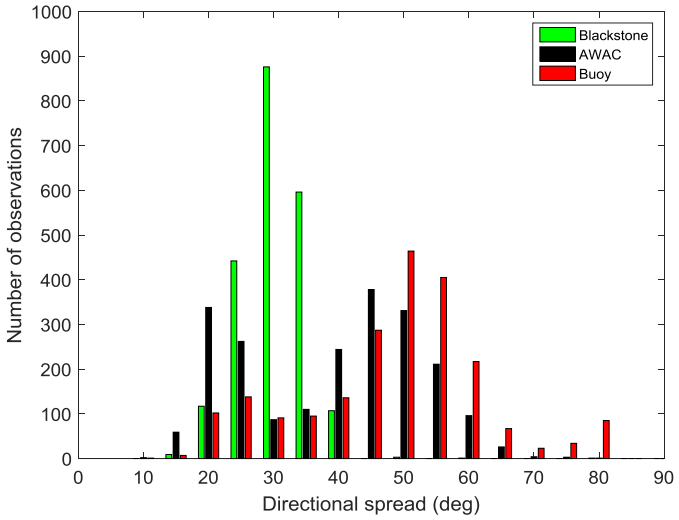

Figure 10 – Histogram of Directional Spread

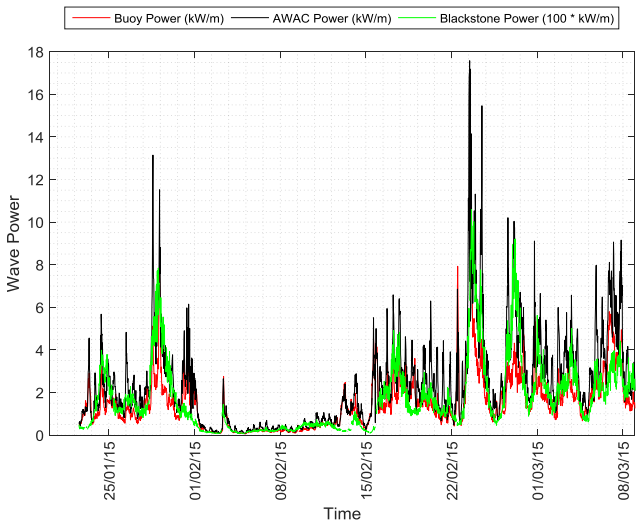

Figure 11 – Wave Power time series

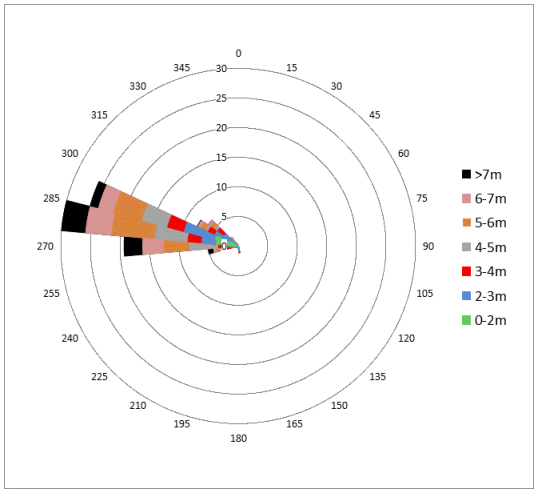

Figure 12 – H_{m0} Percentage Directional Distribution Blackstone Buoy

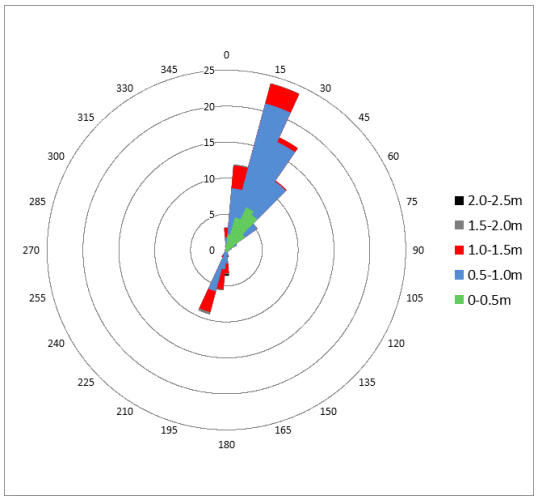

Figure 13 – H_{m0} Percentage Directional Distribution AWAC

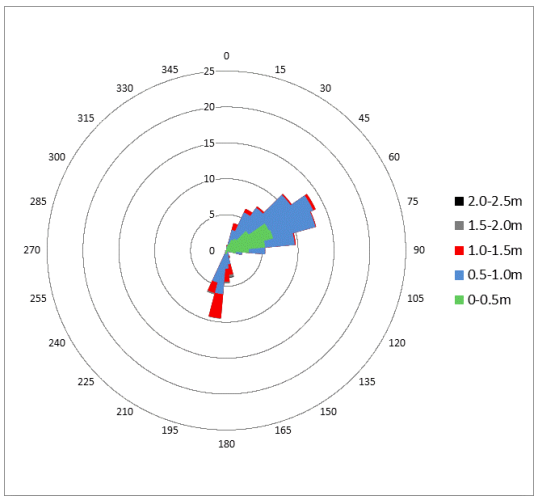

Figure 14 – H_{m0} Percentage Directional Distribution Colonsay Buoy

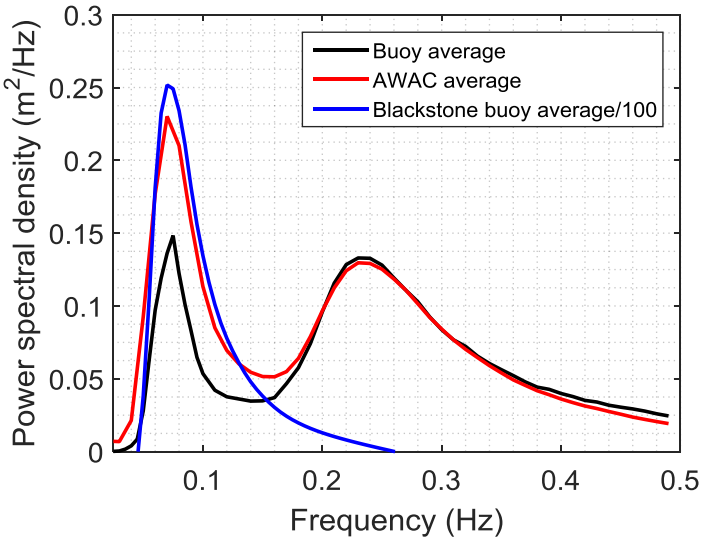

Figure 15 – PSD frequency distribution all sensors

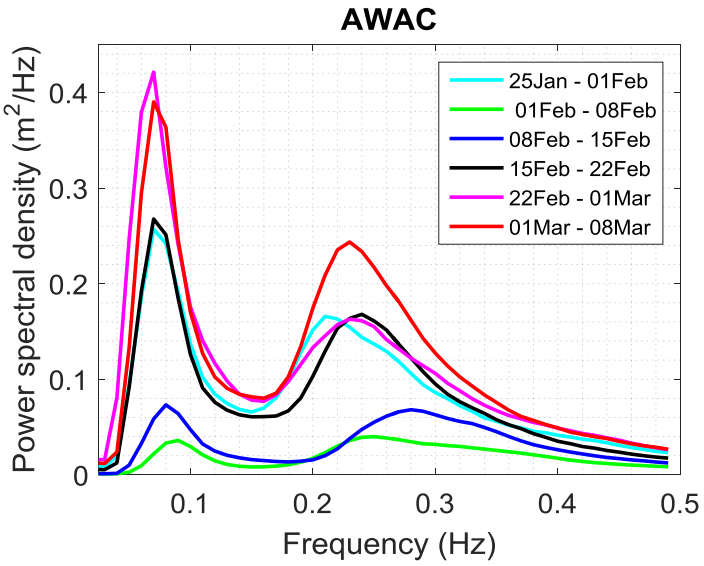

Figure 16 – weekly PSD frequency distribution from AWAC

List of Tables

Table 1 – Sensor detail

Description	Nortek 1 MHz AWAC	Datawell 0.7 m MK3 Waverider Buoy
Measurement principle	Doppler shift; 4 No 1MHz acoustic transducers (1.7° opening angle, 3 beams slanted at 25° from vertical axis and 1 upwards facing for surface tracking)	Double integration of accelerometers in x, y and z direction provides displacement data
Location	Bottom mounted; 1.16 km to the north-east of the buoy; 1.6 km offshore	Surface floating; tethered to mooring via elastic cord 1.25 km offshore
Depth	20 m chart datum	20 m chart datum
Sample rate	4 Hz acoustic; combination of 0.5 h wave bursts and 4 No 60 s averaged current bursts per hour	1.28 Hz continuous
Data access	Internal SD card	Live HF radio link; internal memory card
Auxiliary	Pressure, temperature, compass, pitch and tilt sensors	Temperature, GPS location, compass

Table 2 – RMS error of H_{m0} distributions

Significant Wave Height	RMS error
Blackstone Weibull best fit ($\lambda = 4.2$, $k = 1.7$)	0.0431
Blackstone Rayleigh ($\lambda = 4.3$, $k = 2$)	0.0460
AWAC Weibull best fit ($\lambda = 0.71$, $k = 2$)	0.1693
AWAC Rayleigh ($\lambda = 0.71$, $k = 2$)	0.1693
Colonsay Buoy Weibull best fit ($\lambda = 0.68$, $k = 2.2$)	0.2023
Colonsay Buoy Rayleigh ($\lambda = 0.69$, $k = 2$)	0.2100

Table 3 – Statistical parameters derived from Kernel Density estimation for Significant Wave height

Parameter	Blackstone	Colonsay Buoy	Colonsay AWAC
Bandwidth	0.5102	0.0624	0.07212
Mean (m)	4.501	0.6153	0.6997
Median (m)	4.561	0.5842	0.6896
Standard deviation (m)	1.999	0.2990	0.3188

Table 4 – Statistical parameters derived from Kernel Density estimation for Peak Wave period

Parameter	Blackstone	Colonsay Buoy	Colonsay AWAC
Bandwidth	0.5424	0.9737	0.8267
Mean (s)	13.242	10.206	10.039
Median (s)	13.135	11.964	11.724
Standard deviation (s)	2.603	5.0734	4.516

Table 5 – Average values for wave height, period and power

22/01/2015 13:00 – 09/03/2015 00:00				
	H_{m0} [m]	T_z [s]	T_p [s]	P [kW/m]
Blackstone Buoy	5.45	8	13.2	167
Colonsay Buoy	0.74	3.5	10.2	1.46
Colonsay AWAC	0.84	3.2	10.0	2.36